

Master's Thesis

Classifying attentional dynamics from EEG signals: Feature based perceptual attentional control

Master's Student: Lora Fanda
Student number: 18-696-427

Project Supervisor: Dr. Andre Anjos
Company Supervisor: Dr. Pawel Matusz

Company: HES-SO, Sierre, Vallais

Copyright: All rights reserved

Date: February 12th , 2021

Abstract

The general goal of this project is to understand if something as generic as paying attention to visual stimuli, whether intended or driven by distractor objects, can be classified well. People's ability to behave effectively in everyday situations is critically dependent on "selective attention", which is the ability to promote the processing of objects that match our current behavioral goals and suppress those objects that do not match those goals. The last decades have provided significant advances in terms of brain and cognitive mechanisms orchestrating selective attention as well as their role in enhancing perception and supporting the learning of new information. However, this knowledge of both processes of intended and distracted attention has yet to be discriminated. **Goal:** If distraction and intention can be classified by only neural input, particularly in real-world, multisensory environments, this could bring forth knowledge of the underlying differences in mechanisms additive to the traditional neural analysis methods. For this reason, it is particularly useful to model and understand cognition processes through statistical modelling, such as those in Machine Learning (ML) applications on attentional control data. **Methodology:** In particular, employing ML techniques to discriminate between visual selective attention to *distractor objects* vs. *intended object*, in an unbiased and automatic manner, without relying on subjective evaluation. **Results:** In this endeavor, a linear classifier was trained to successfully classify attention to distractor object, intended object, or neither, with the best accuracy score of 0.65 (chance accuracy score = 0.33). Additionally, the selection of features from N2PC regions resulted in the best accuracy score of 0.65 while decreasing feature size to 10.9 percent of total features (14/128 electrodes). However, the non-N2PC region features suggested that attention is a process that uses whole-brain activity.

Acknowledgement

I would like to express my deepest appreciation to my supervisors, Andre Anjos and Pawel Matusz, for the invaluable guidance throughout this Masters.

I would also like to extend my deepest gratitude to Henning Muller, for his continued support and valuable advice, and to Micah Murray, for the opportunity to advance my learning.

I would like to extend my sincere thanks to Olivier Bornet, and all teachers and mentors of IDIAP and UniDistance, who have made it possible for me to arrive at this point. The road was difficult, and I am very grateful for all your help along the way.

I would like to thank Yashin DiCente Cid, for the profound belief in my abilities and the helpful advice and guidance. I am also grateful to all coworkers at HES/SO, for constructive advice and insightful suggestions.

A very special thanks belong to Davide Calvaresi, for all the love and support in the past year, making my success that much more possible.

Last but not least, my deepest love and gratitude to my parents, Syndyse Abedini and Fatmir Fanda, who taught me to be strong in the face of difficulties, and to my little sister Lisa, who sent me the warmest hugs, all the way from New Jersey, whenever I needed them.

Contents

1	Introduction	11
1.1	What is Attention?	11
1.1.1	Selective Attention	12
1.1.2	Visual Selective Attention	12
1.1.3	Measuring Attention	14
1.2	Why classify Attention?	16
1.3	Why ML?	17
1.3.1	Classifying Neural Data	17
1.4	Summary	18
2	State of the Art	20
2.1	Attention in Neuroscience	20
2.1.1	Brain Activity Acquisition: EEG	20
2.1.2	EEG	21
2.1.3	N2PC	21
2.1.4	Visual Selective Attention to Intended Objects	22
2.1.5	Visual Selective Attention to Distractor Objects	22
2.1.6	Summary of Attention in Neuroscience	22
2.2	Machine Learning for Classifying Neural Signals: Non-Attention based	23
2.2.1	BCI	23
2.2.2	Epilepsy	25

2.3	Machine learning for Attention	26
2.3.1	LDA with N2PC signal amplitude	26
2.3.2	SVM with MEG signal amplitude	26
2.3.3	LDA with N2PC signal amplitude	27
2.3.4	Summary	27
2.4	Working Hypotheses	27
3	Data, Methods, & Experimental Setup	29
3.1	Data	29
3.1.1	Data: Paradigm	29
3.1.2	Data: Acquisition	31
3.2	Methods	31
3.2.1	Preprocessing	31
3.2.2	Feature Extraction	33
3.2.3	Data Visualization	35
3.2.4	Dimensionality Reduction	36
3.2.5	Dataset Normalization	37
3.2.6	Classification	38
3.3	Experimental Setup	39
3.3.1	E1: Classifying frequency domain features	39
3.3.2	E2: Classifying N2PC and non-N2PC Region features	40
3.3.3	E3: Identify which class is the most separable	42
3.3.4	E4: Dimensionality Reduction to strengthen decisions to re- ject or not reject hypotheses	43
4	Experimental Results	45
4.0.1	R1: Classifying frequency domain features	45
4.0.2	R2: Classifying N2PC and non-N2PC Region features	48
4.0.3	R3: Identify which class is the most separable	50
4.0.4	R4: Dimensionality Reduction to strengthen decisions to re- ject or not reject hypotheses	53

5 Discussions	55
5.1 Hypotheses	55
5.2 Discussion of Results	56
5.2.1 D1: Classifying frequency domain features	56
5.2.2 D2: Classifying N2PC and non-N2PC Region features	57
5.2.3 D3: Identify which class is the most separable	57
5.2.4 D4: Dimensionality Reduction to strengthen decisions to reject or not reject hypotheses	58
5.3 Hypotheses rejected or not rejected	58
5.3.1 Discussions Summary	59
5.3.2 Limitations:	60
5.4 Conclusion	61

List of Figures

1.1	Components of Selective attention. This figure illustrates the 5 senses attention is driven by and in particular shows the division of visual attention into further components; spatial and feature-based visual selective attention. Feature-based attention is the focus of the thesis, which is further defined by the intended object and distractor object.	13
1.2	Spatial and Temporal resolutions of commonly use brain activity measurement tools: Source of image: [37].	14
1.3	Temporal importance: Given 0 is stimuli onset, this figure illustrates the delay in activation of all components in attention. C1, N1, and P1 are sensory components (non-selective attention) and N2PC, ADAN, and LDAP are target selection components (selective attention). Figure 3.1 shows how this temporal region translate to the dataset's paradigm, with only N2PC application to each stimuli (none, distractor, or intended object) onset. All components have been plotted in a time-line to visualise and highlight the latency in the selective attention activation for target selection components, information taken from many sources [20, 5, 34, 13, 15, 23].	15
1.4	Cortical activity spatial variability in 5 example processes. Visualization of meta-analysis maps of motor, touch, auditory vision, and attention maps, to show the variable spatial presence differences between each map/process. Motor, Touch, Auditory, Vision, and Attention all have different activity maps, yet attention seems to have the least "hub" like activity map. This series of brain images were generated using EduCortex [42], which visualizes fMRI mega-analysis maps based on specific term searches.	16
1.5	General Supervised classification procedure. (A) A classifier is trained from a labeled training set to output a trained model. (B) a new, unseen testing set is used to <i>evaluate</i> the trained model's performance by inputting an unlabeled training set and comparing the predicted labels to true labels for a model accuracy measure.	18

2.1	This figure illustrates the main steps involved in EEG data collection. Here, Matteo participating in a research study by responding on the laptop. The behavioral data (for example: response time, correct trial) is saved locally or transferred to the Data Acquisition System. Additionally, in order to measure cerebral activity, Matteo is wearing the noninvasive EEG cap and neural activity in the brain are recorded.	21
3.1	This figure shows all 4 stimuli of the paradigm (A - D) and the time importance of the three interested regions. (A) is "Baseline" Class 0, (B) is "Cue" Class 1, and (D) is "Target" Class 2 stimuli. The cross (C) is not used in this study. Additionally, (E) shows the temporal distribution of the N2PC components for the 3 selective attention stimuli (Distractor object = Cue, Intended object = Target, and no attention = Baseline).	30
3.2	Overview of the complete preprocessing procedure , from data acquisition to feature vector formation. (A) is the preprocessing performed in Cartool [2], (B) is further preprocessing and restructuring of the dataset for the purpose of the projects goals see, and (C) is the feature extraction with DCT).	32
3.3	Using Cartool software, the standard EEG preprocessing is applied, followed by extracting EEG data of interest. (A) whole experiment, (B) time intervals of interest (Baseline, Cue, and Target) within each trial, for each participant, and (C) splitting each trial (of 600 ms) into 3 data samples (150 ms each) with appropriate labels (Baseline, Cue, Target), then reordering and splitting into train, test, and validation sets. (Distractor object = Cue, Intended object = Target, and neither = Baseline).	34
3.4	Acquired EEG data vs last stage of preprocessing, results , visualized with MNE [31]. The plot shows all EEG electrodes (128) for one trial of the experimental acquisition, in butterfly view (all electrodes centered at 0 microV). Difference between the figures is a result of (i) removing bad electrodes (gray signals), (ii) interpolation and (iii) filtering for 50 Hz noise.	36
3.5	EEG Cap images showing the regions of interest (from left to right) of a full electrode coverage, N2PC regions (E2.a Electrodes) in red, non-N2PC regions (E2.b Electrodes) in blue, and the lack of overlap between N2PC and non-N2PC regions.	41
4.1	Classification of DCT[1,49], DCT[50,99] and DCT[100,149] using LR and SVM classifiers. The <i>average</i> performance accuracy from the 10 fold cross-validation is plotted for each DCT component range. LR in blue, SVM in green.	46

4.2	Classification of DCT: LR and SVM classification results as <i>average</i> performance accuracies from the 10 fold cross-validation for DCT[1,49] to DCT[1,99] and DCT[1,149]. LR in blue, SVM in green. The <i>maximum</i> performance accuracies for [LR,SVM] are [0.60,0.60], [0.61,0.62], [0.65,0.65] for DCT[1,49] to DCT[1,99] and DCT[1,149], respectively.	46
4.3	Performance (accuracy scores) of LR and SVM over 10-fold cross validation.	47
4.4	Figure showing (mean,standard deviation) of the training set, validation set and test sets. The top graph shows the mean (at x = 0) and standard deviation (x = 1 range) of the Train (black/grey), validation (red/pink), and test (light blue/blue) datasets. The bottom three graphs are for each Train Validation and Test set, showing the distribution of features in each class; Baseline (gray), Cue (red), and Target (Blue).	48
4.5	Classification Accuracy scores between LR and SVM on (A) all electrodes, (B) N2PC electrodes, (C) and non-N2PC electrodes, for Baseline = 0, Cue = 1, and Target = 2.	49
4.6	Confusion Matrices of LR and SVM over 10 fold cross validation. The accuracy scores are shown for each class true labels (y axis) and predicted labels (x axis), for Baseline (Class 0), Cue (Class 1), and Target (Class 2). This figure follows the accuracy scores visualized in Figure 4.3.	50
4.7	Weight Coefficients of LR model: Overview of trained LR model coefficient to look for patterns. Since there are 128*149 features, it is difficult to plot everything. Hence, we used two examples. Bar-plot (A) shows coefficients for DCT bin 10 for electrodes 64 to 95, and (B) shows coefficients for Electrode 65 for DCT 1 to 49.	51
4.8	Classifier predictions for Baseline (Class 0), Cue (Class 1), and Target (Class 2). Top graph is training data, bottom graph is validation data.	52
4.9	Figure showing LDA dimensionality reduction to training set (row 1) and validation set (row 2).	53
4.10	Figure showing PCA dimensionality reduction performance. (A) Accuracy scores on the validation set over various percentages of variances contained. (B) Confusion matrices for LR applied without (left) and with (right) PCA dimensionality reduction. Dotted black line is comparative LR performance accuracy.	54

5.1 Figure illustrating the work-flow from background knowledge to rejecting or failing to reject the 4 hypotheses. The discussion of the experimental results which lead to the conclusions seen in this figure are explained in Section 5.2. 56

List of Tables

4.1	Table of <i>Average</i> Classification Accuracy scores for the 10 fold cross-validation between LR and SVM on <i>(i)</i> all electrodes, <i>(ii)</i> N2PC electrodes, and <i>(iii)</i> non-N2PC electrodes	50
5.1	Table of Classification Accuracy score summaries, between other selective attention studies, as well as other BCI and Epilepsy classification studies.	59
5.2	Table of Experimental results of classification performance accuracy across the experimental setups. For PCA, (*0.95) indicates 0.95 of the variance contained.	60

Chapter 1

Introduction

“Attentional Blindness” is a general term for any failure to identify stimuli that should possibly be attributed to attentional factors *rather than* perceptual impairment [11]. Comprehending attentional dynamics can help improve the ability to differentiate between visual stimuli attributed to attentional factors or perceptual impairments. Cathy Davidson, founder of Duke University’s Center for Cognitive Neuroscience and the author for “Now You See It”, shows that “attention blindness” has produced one of the most challenging problems of our society [10]. She believes that the expectation of what real-world attention is (or isn’t) and how it reflects intelligence leads to diminishing the number of students who do not fit the mold that is currently defined by attention or intelligence. Thus, when the students do not fit the mold, they are deemed as failures. Fortunately, the more we understand about the concept of attention and how it manifests neurally and behaviorally, the closer we are to eliminating engraved biases and supporting adapted attention and intelligence relations.

1.1 What is Attention?

In psychology, attention is distinguished into three processes – alerting, orienting, and selective attention. When attention is studied, it is generally the selective attention process that is studied. From now onward, attention and selective attention will have the same meaning for this thesis.

Attention is the process in which limited computational resources are flexibly hired to perform a task. The concept of attention, whether applied to Machine Learning (ML) or neuroscience, is quite similar. Much like in Artificial Neural Networks (ANNs), biological attention uses parallel processing subsystems, where each unit system has an input and output role that feeds to the following unit

system and so on until completion; Completion in ML is the decision reached while in neuroscience it is the behavioral response.

In nature, attention is forced to be a selective process. The amount of overall energy consumption available to the brain is limited and constant[4], even though the allocation of this energy is flexible according to the specific task demand. Thus, the limitations in energy and concurrently engaged processes led to the idea that selective attention arises from the brain's limited information processing capacity[4]. Thus, stimuli compete for the limited resources in the brain, a hypothesis known as the “biased-competition hypothesis” [12].

1.1.1 Selective Attention

The “biased-competition hypothesis” gives rise to selective attention. In daily interactions with the real world, neural representations encode information about the world (movements memories emotions, for example) from which a competitive cortical process selects the salient occurrences. This form of selective attention creates a successful interaction with the environment. As previously stated, in neuroscience, cognitive science, and psychology, attention is activated selectively, depending on specific sensory inputs or a group of sensory inputs as dictated by the bias-competition hypothesis. In other terms, selective attention is defined by *bottom-up* processing or *top-down* processing. Bottom-up processing is salience-driven attention (attentional processing driven by the properties of the objects themselves), and top-down processing is goal-driven attention. For example, Bottom-up attentional resources are captured to the location of an unexpected bright light, these processes are pre-conscious, or non-volitional responses [33]. Top-down processing includes executive attention, which means attention orienting is under the control of the person who is attending and what they currently intend to accomplish (i.e., the task at hand) [6].

As we are interested in understanding feature-based attention to distractor or intended objects, the top-down attention is the focus of this thesis.

Naturally, selective attention is a multisensory process, in which all five sensory modalities are activated in competition with each other to accomplish a task or be aware of the surroundings [33]. The five sensory modalities are visual, tactile, auditory, gustatory, and olfactory. In this thesis, the focus is on *visual* selective attention.

1.1.2 Visual Selective Attention

One such sensory driven attention is visual attention, which is further defined by visual *spatial* attention and visual *feature-based* attention. Visual-spatial attention

is driven by the salience of objects, which means attention is captured to objects move or have a particular presence such as shine, loudness, or distinct color (i.e., bottom-up attention). Visual *feature-based* attention is driven by similarities in features of the intended object, which means attention is captured when objects include features similar to the intended object (such as color, shape, and shine in distractor objects), or are they intended object themselves. This hierarchy, starting from selective attention and for this thesis, is best visualized in Figure 1.1.

For a conceptual parallel, *visual spatial attention* can be thought of as with unsupervised learning as selective attention happens without prior knowledge (i.e., no labels), and visual feature attention can be paralleled with supervised learning. The participant learns some features of the intended search objects which are connected to certain targets (i.e., labels). Thus, distractor objects can have selective attention abilities due to visual feature attention during selective attention. Similarly, intended objects can have selective attention due to feature attention, and additionally, due to temporal attention and pre-motor attention, depending on the completion requirements of the task (to grasp an intended object, for example).

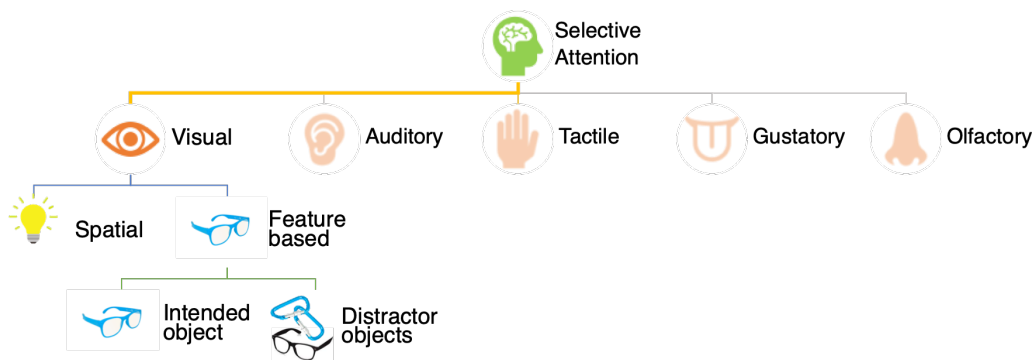


Figure 1.1: **Components of Selective attention.** This figure illustrates the 5 senses attention is driven by and in particular shows the division of visual attention into further components; spatial and feature-based visual selective attention. Feature-based attention is the focus of the thesis, which is further defined by the intended object and distractor object.

Following Figure 1.1, let us consider an example to better illustrate visual selective attention: Say you have lost your blue glasses and you would like to search for them. You enter your bedroom as you believe that was the last place you saw them and you start your search through your room. While searching for your blue glasses, your blue climbing carabiners on your desk distract you (feature-based attention to distractor object). In the end, you finally find your blue glasses (feature-based attention to the intended object) on your desk.

In the previous example, since you had a task at hand (i.e. to find blue glasses), your attention was classified as *Feature-Based Visual Attention*, where the *Intended*

Object was your blue glasses and the *Distractor Objects* were other objects with similarity to color, shine, or shape. to your intended object. *Whenever* you diverted your attention to the distractor objects, your attention was *Feature-Based Visual Attention* to distractor objects. In parallel, *whenever* you diverted your attention to the intended object, your attention was *Feature-Based Visual Attention* to the intended object.

1.1.3 Measuring Attention

Two very important driving factors in deciding how to measure and acquire brain activity data are *Spatial* and *Temporal* resolution. The higher the resolution both temporally and spatially, the better the data acquisition. For measuring Selective Attention, a high temporal resolution is important, whereas a high spatial resolution is less critical.

Electroencephalography (EEG) and Other Tools

As analyzing selective attention requires a high temporal resolution with a decent spatial resolution, Electroencephalography (EEG) is an ideal method for data acquisition. In Data and Methods (Chapter 3), the paradigm and data acquisition methods are explained in further detail.

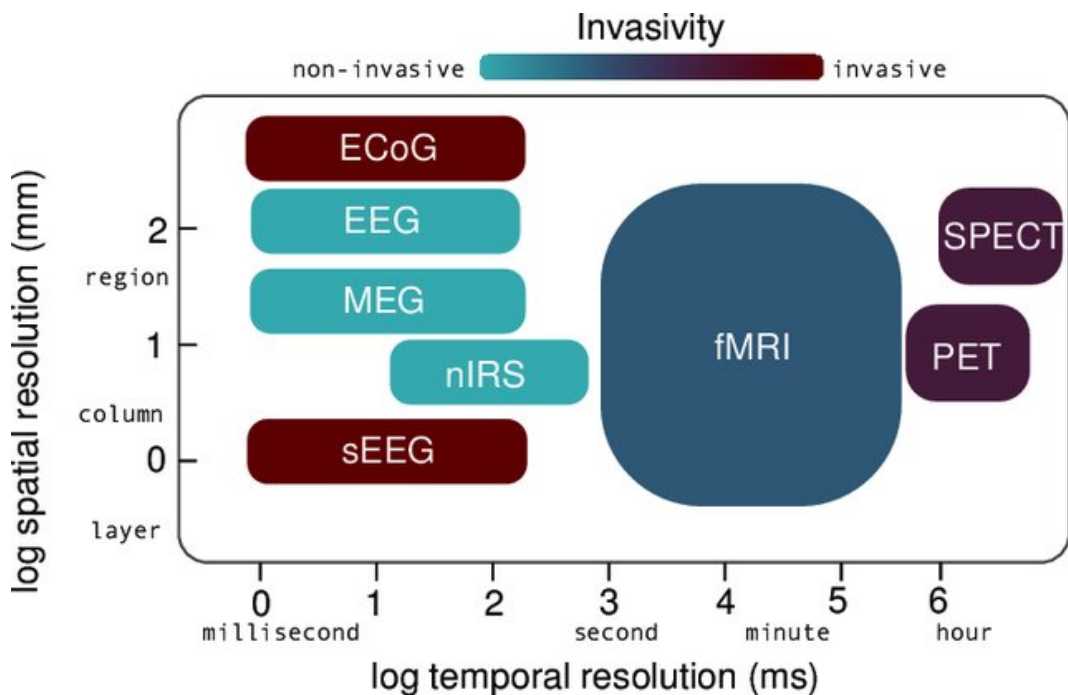


Figure 1.2: **Spatial and Temporal resolutions of commonly use brain activity measurement tools:** Source of image: [37].

In addition to EEG, other methods of data acquisition for the analysis of *attention data* include Magnetoencephalography (MEG), functional magnetic resonance imaging (fMRI), and Electrocorticography (ECoG). Other methods of data acquisition for the analysis of brain activity in general include Local Field Potentials (LFPs), Positron emission tomography (PET), and computed tomography (CT). Figure 1.2 compares the spatial and temporal resolution of some of these methods of cortical data acquisition [37].

Temporal Importance

Selective attention is a process that occurs in delay, meaning it has a latency in its activation. Understanding the “temporal mapping” of selective attention is imperative for (i) appropriately understanding if the tool selected has a necessarily high enough temporal resolution and (ii) to understand which are the temporal regions of interest in the acquired dataset.

Temporally, components of attention are mainly grouped into the sensory components and target selection components. Sensory components include the first component to respond to visual stimuli (C1), the first positive-going component of attention (P1), the negative-going component to unpredictable stimuli (N1). Target selection components include the negative-going posterior-contralateral component of selective attention (N2PC), gaze-congruent anterior directing attention negativity(ADAN), and late directing attention positivity (LDAP).

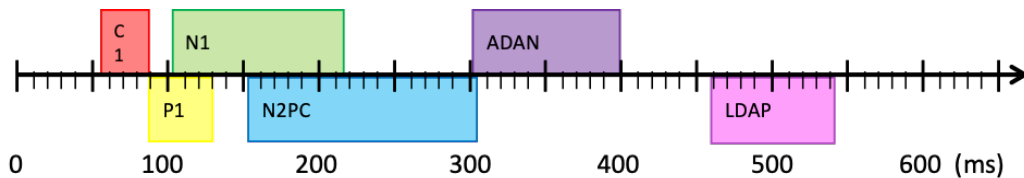


Figure 1.3: **Temporal importance:** Given 0 is stimuli onset, this figure illustrates the delay in activation of all components in attention. C1, N1, and P1 are sensory components (non-selective attention) and N2PC, ADAN, and LDAP are target selection components (selective attention). Figure 3.1 shows how this temporal region translate to the dataset’s paradigm, with only N2PC application to each stimuli (none, distractor, or intended object) onset. All components have been plotted in a time-line to visualise and highlight the latency in the selective attention activation for target selection components, information taken from many sources [20, 5, 34, 13, 15, 23].

Figure 1.3 shows a temporal mapping of the main components of attention. Assuming 0 is stimuli onset, the early components of visual stimuli response (C1, P1, N1) are elicited by the processing of stimulus physical features [20, 5, 34, 13]. Target selection components (N2PC, ADAN, and LDAP) are processed later and reflect selective attention. Target selection components are the regions that index selective attention, with particular importance going to N2PC, which indexes selective attention of *distractor objects* [15] and of *intended objects* [23].

Spatial Importance

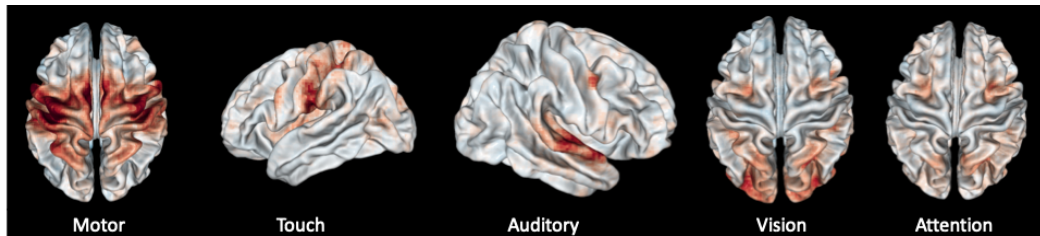


Figure 1.4: **Cortical activity spatial variability in 5 example processes.** Visualization of meta-analysis maps of motor, touch, auditory vision, and attention maps, to show the variable spatial presence differences between each map/process. Motor, Touch, Auditory, Vision, and Attention all have different activity maps, yet attention seems to have the least "hub" like activity map. This series of brain images were generated using EduCortex [42], which visualizes fMRI mega-analysis maps based on specific term searches.

It is important to understand spatial regions of attention associated with attention for data acquisition and analysis. If one does not know where electrodes should be placed, the data collection would be less valuable, and so the experiment. Figure 1.4 shows the spatial variance in the activity of sensory processed, including attention. This helps contrast and understand the non-regionally specific nature of attention, important to keep in mind when features are selected in electrode settings.

In figure 1.4, there are five brain maps taken from EduCortex, a visualization software developed by Scotti et al [42] allows for search terms then indicates, with sources, where the regions of activity are for those terms. Here, there are *five* terms – Motor, Touch, Auditory, Vision, and Attention. This explains the difference between attention and the other *four* sensory mechanisms (Motor, Touch, Auditory, Vision) terms' spatial neural response.

On the one hand, sensory mechanisms have an activity "hub" in a specific region. Motor and touch are in the premotor and sensorimotor regions. The auditory is in the auditory cortex. Vision is in the visual cortex. In contrast, attention does not have a strong activity "hub", in part because of the complex composition of attention, and additionally because attention has a latent response and by nature is not as strongly evoked as a sensory stimulus. However, from Figure 1.4, it is visible that attention encompasses a large spread of surface activity (such as sensory-motor regions and visual cortex). This is important to keep in mind for electrode analysis and feature extraction, and to compare with other BCI and Ictal (i.e., Epileptic) activity classification tactics in the later chapters.

1.2 Why classify Attention?

The last decades have provided important advances in terms of brain and cognitive mechanisms orchestrating selective attention as well as their role in enhancing

perception and supporting the learning of new information [23, 33, 30, 45]. The presence and nature of selective attention to distractor objects [23] and intended objects (in literature, coined as “target” objects) [15] is well understood and studied. However, this knowledge is limited, as the processes of *intended* vs. *distracted* attention have yet to be discriminated from each other.

If distraction and intention (target selection) can be classified by only neural input, particularly in real-world, multisensory environments, this could bring forth knowledge of the underlying differences in mechanisms. Additionally, this would further the knowledge regarding selective attention, as traditional neural analysis methods are limited since they *cannot* reveal the underlying brain mechanisms. For these reasons, it is particularly useful to model and understand cognition processes.

1.3 Why ML?

Now that the main aspects of selective attention and its relations to everyday functioning are understood, it is time to understand how ML is employed in attention mechanisms and in other time-series brain activity data.

To help a model distinguishing between selective attention to distractor objects or intended objects automatically and objectively, it is necessary to understand (i) the attributes of selective attention signals and (ii) how to incorporate ML in the application of cortical signals.

Previous literature in section 1.1 has highlighted the main attributes of selective attention and defined the types of attention this thesis is attempting to discriminate between. Furthermore, it is important to understand *how* ML is incorporated to discriminate between *distractor* and *intended* selective attention .

1.3.1 Classifying Neural Data

To discriminate the type of attention, classification is generally employed. Assuming you have an input signal (in this case, EEG) and a label associating it (in this case, Distractor, Intended, or Neither), you can train an ML classifier to classify the neural information into one of the labels. Thus, when new, unlabeled information is presented, the model can predict which label the neural information most likely belongs to. This process is explained in Figure 1.5.

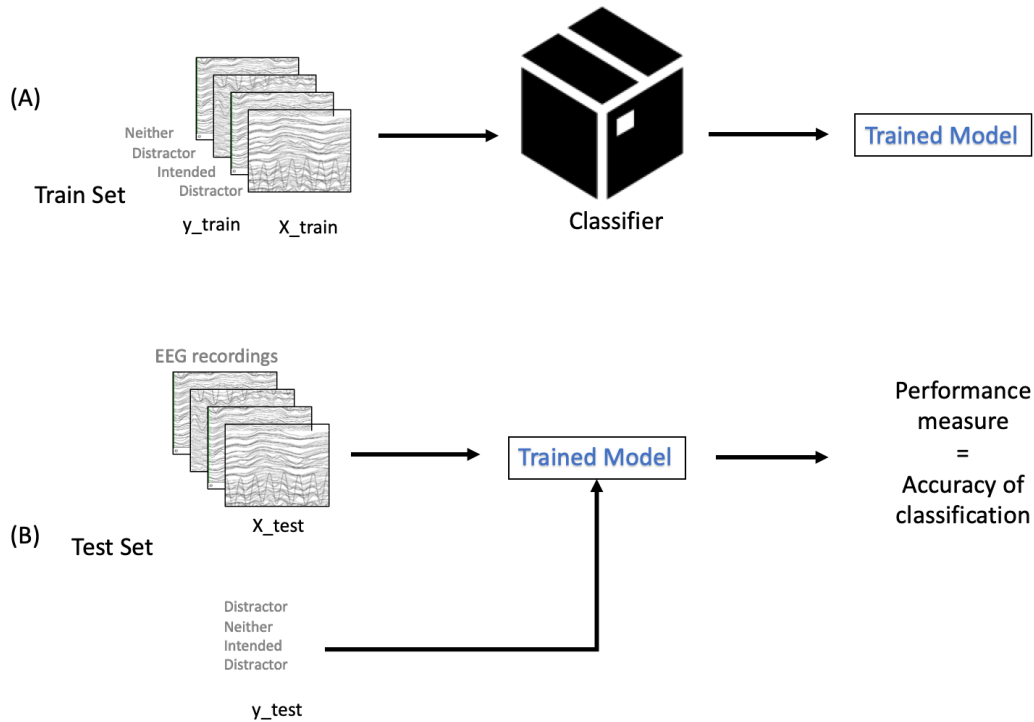


Figure 1.5: **General Supervised classification procedure.** (A) A classifier is trained from a labeled training set to output a trained model. (B) a new, unseen testing set is used to *evaluate* the trained model's performance by inputting an unlabeled training set and comparing the predicted labels to true labels for a model accuracy measure.

Data Knowledge

To accomplish the classification of three types of attention, we will use EEG acquired neural recordings from 39 participants performing a selective attention paradigm. This dataset was collected by Dr. Turoman [45]. This dataset will follow standard preprocessing procedures of EEG data as mentioned in Turoman et al [45], additional preprocessing required by ML approaches to identical and similar time-series datasets [29, 28] and standard ML approaches which have been used previously in similar datasets for other cortical activity classification applications [17, 46, 32].

Chapter 2 dives into the state of the art of current classification techniques for brain activity data of various aims and later focus on classification applied to specifically attention and N2PC components.

1.4 Summary

Thus, understanding how attention attributes are neurologically and behaviorally portrayed, and therefore how well-intended or distractor attention can be clas-

sified can help fine-tune the understanding of selective attention in real-world setting such as in educational systems. Naturally, understanding attention leads to redefining and further understanding “intelligence” in association to attention, and hopefully attempting to minimize the blindness towards the concept of attention that Dr. Davidson addresses [10].

This much-needed insight in understanding and classifying attentional control is beneficial to all ages in all learning environments, including workplaces. For this reason, it is particularly useful to model and understand cognition processes through means ML, as they can aid in creating a model that can discriminate the type of attention (distractor, intended, or neither/baseline) once presented with an organized and labeled training set.

This aim falls in parallel with the goals of Group for Real World Neuroscience (GROWN), led by Dr. Pawel Matusz, and the MedGIFT group, led by Dr. Prof. Henning Muller, at University of Applied Sciences Western Switzerland (HES-SO). GROWN aims to utilize neuroscientific knowledge and tools to improve and better understand people's daily functioning in real-world environments, and therefore improving their quality of life.

Chapter 2

State of the Art

The objective of this thesis is to find a method that is fast, objective, and can distinguish the type of attention. Therefore, we aim to apply ML techniques to objectively determine the type of attention, without relying on subjective evaluation.

As the goal of this thesis is to apply ML techniques to objectively determine the type of attention, it is imperative to understand the state of the art in the Visual Selective Attention to Distractor and Intended objects, in both fields of neuroscience (context) and machine learning (classification). For this reason, the state of the art is divided into 3 main sections to cover all current knowledge in the respective fields:

- (i) Attention in Neuroscience: Visual Selective Attention
- (ii) ML for Cortical Signals: Cortical Signal Classification
- (iii) ML in Attention: Classification of Attention
- (iv) Relevant ML Concepts
- (v) Working Hypotheses Summary

2.1 Attention in Neuroscience

2.1.1 Brain Activity Acquisition: EEG

Selective attention has been studied using various modes of data collection, ranging from fMRI, PET, ECoG, to EEG [24, 37, 3, 4]. To understand how these attentional features can be captured, both in temporal and spatial domains, we must understand different methods of data acquisition. Previously, in chapter

1, we highlighted the importance of high temporal resolution and decent spatial resolution for neural recordings for selective attention . For this reason, we stated EEG is an ideal technology for the study of attention and attentional dynamics. Thus, EEG neural recordings of three types of selective attention (Distractor object, Intended object, and neither) are used to classify selective attention.

2.1.2 EEG

EEG is a tool used to monitor and record electrical activity of the brain, which is resulting from the currents within the groups of neurons in the brain [35]. This electrophysiological monitoring method is non-invasive (see Figure 1.2), with electrode varying electrode density designs. The electrodes that monitor the electrical activity are placed on the surface of the head as a cap, with a similar spatial orientation of the electrodes as seen in Figure 3.5. For a visual representation of EEG data collection, see Figure 2.1.

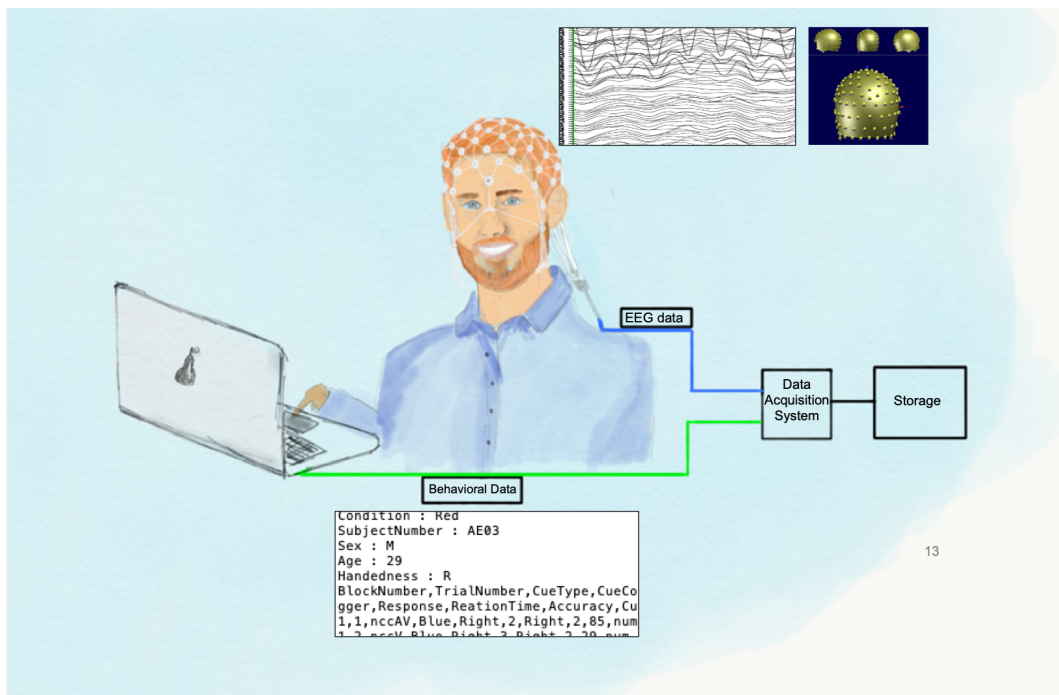


Figure 2.1: This figure illustrates the main steps involved in EEG data collection. Here, Matteo participating in a research study by responding on the laptop. The behavioral data (for example: response time, correct trial) is saved locally or transferred to the Data Acquisition System. Additionally, in order to measure cerebral activity, Matteo is wearing the noninvasive EEG cap and neural activity in the brain are recorded.

2.1.3 N2PC

N2PC is cortical measure of suppression of distractor object during a selective attention process. This is valuable, as involuntary vs. voluntary attention informs

us about the distractor objects' ability to diverge attentional control. N2PC, a well-understood event related potential (ERP) correlate of selective attention of potentially task-relevant objects. N2PC is reflected by an enhanced negativity 200ms over posterior electrodes contralateral to the stimulus location and it is known to be modulated by top-down visual attention processes. In simpler terms, N2PC activity is seen 150ms after stimulus onset and has a negative-going measure.

2.1.4 Visual Selective Attention to Intended Objects

Additionally, Nobre et al [7] confirm the presence of changes in the ERP strength over N2PC time period triggered by visual intended (target) objects where attention was captured in visual targets. Additionally, they are able to identify equivalent N2PCs when target items were identified within a memory representation. They were able to duplicate this findings in N2PC analysis of child participants of a visual search task[16]. Overall, this shows that N2PC is a good measure of selective attention to intended (target) objects.

2.1.5 Visual Selective Attention to Distractor Objects

It turns out that the properties of the intended object that we decide to use to define it by, and so search by, are the driving factors that determine the selective attention to *distractors*. This was initially shown in a study by Eimer et al. [15] and further supported ever since [45, 33]. The nature of the paradigm is similar to ours, where the participants were asked to search for a color-defined target, but the target was preceded by an array of different objects (distractors). Similarly, the paradigm from Turoman et al. used target-defining features so that feature-based attentional control guides the selective attention of objects in space [45], where the aim was to study distractor object selective attention in multisensory settings. Among other results, they were able to notice selective attention to distractor objects, using traditional N2PC methods and novel Electrical Neuroimaging (EN) analysis. Thus, this justifies us to try to test if we can classify attention to distractor from that to target.

2.1.6 Summary of Attention in Neuroscience

There is a benefit to being able to distinguish a distractor selective attention to an attentional object capture. For this, applying a classification protocol to a paradigm similar in nature to the Folk et al. [18] task set contingency capture paradigm can give insight on if the attentional dynamics behind the selective attentions, whether to distractors or intended objects, can be distinguished.

N2PC is a marker of selective attention, which is measured using EEG methods. Hence, the N2PC is well suited as an index of attentional processes towards visual stimuli of distractor or intended objects. Turoman et al. [45] confirmed that changes in the ERP strength over the N2PC time period (but not in the traditionally-used N2PC amplitude) triggered by visual distractors predicted behavioural effects across tasks where attention was captured in visual targets. Additionally, Nobre et al [7] confirm the presence of changes in the ERP strength over N2PC time period triggered by visual intended objects where attention was captured in visual targets.

Therefore, the presence of attentional control is supported for both distractor and intended objects, and the next natural step is to identify if it is possible to train a classification algorithm to successfully classify distractions from intended attentional control while also considering a baseline condition. To do so, a proper understanding of classification paradigms applied to cortical activity need to be understood. Section 2.2 focuses on classifying neural signals, and further emphasis on selective attention classification is focused on Section 2.3.

2.2 Machine Learning for Classifying Neural Signals: Non-Attention based

Neural Signal Classification had been investigated primarily in two different research areas:

- 1 **Brain Computer Interfaces (BCI)**: BCIs aim to translate brain activity into a command using regression or classification algorithms [28, 29].
- 2 **Epilepsy**: Classification of Ictal (i.e. Epileptic) activity, likely real-time for seizure monitoring[3, 36].

2.2.1 BCI

BCIs translate brain activity into a task-specific command using regression or classification algorithms. Much like EEG attention data, BCI features can be noisy and likely contain outliers [47], thus requiring regularization. However, various experiments in BCI applications show that both simpler linear models [39] and more complex [19] non-linear models accomplish good classification results, which is a promising find. It is important to note that, although EEG can have a low signal-to-noise ratio, it is possible to extract discriminative information to classify with even simple linear models.

Classification

From literature [28, 29, 39, 47], the classifier with promising results for multi-class classification is suggested to be performed with Support Vector Machines (SVMs). Additionally, using EEG recorded neural signals, SVM classifiers were easily able to learn even while using raw EEG data [21]. It is important to note that this was a binary classification task.

An additional method used was the employment of Dynamic classifiers for BCI's. Dynamic classification is applied to the temporal features of BCI data, where for each temporal feature, classifiers are selected dynamically. Dynamic classifiers are beneficial, particularly if temporal information is necessary to contain [28]. Containing time information is not essential for the goals of this thesis, and this information is therefore not further applied or discussed.

Features

A few groups applied classification algorithms to directly raw EEG data for BCI applications [21, 28].

Frequency features: Likely the most relevant application of BCI to the selective attention goal is the consideration of extracting features from several time segments, which is what Pfurtscheller et al. [38] did. Their task was to discriminate between the imagination of right, and left-hand movements from EEG acquired dataset. To use temporal information like frequency components, they extracted such information from each desired time segment and concatenated relevant information to form one feature vector. A promising feature for extracting frequency components of signals in desired time regions is using Discrete Cosine Transform (DCT) on a MEG dataset [22].

Raw EEG features: Direct use of the EEG dataset have previously been done. Raw EEG values, without further preprocessing or extraction, have previously been used. Kaper et al. have used raw EEG values in Gaussian SVM classification for an accuracy of 1.0 in a competition task [21]. Additionally, Zhang et al. have used amplitude values of Smoothed EEG for linear SVM and LDA with accuracy of 0.926 and 0.907, respectively [47].

AutoRegressive features: In order to find spectral features that best separate the data while keeping the accuracy relatively high, AutoRegressive (AR) feature selection is a solution. Via AR, Garrett et al. learn the best dissociating spectral features for a given subject and task, then used the trained LDA, NN, and SVM with the best dissociating features in real-time. Their accuracy results were 0.66, 0.694, and 0.72, respectively [19]. Schlogl et al. applied adaptive AR to use in spectral properties of the EEG, using k-nearest neighbours classification, LDA, and SVM, for an accuracy of 0.42, 0.54, and 0.63, respectively [39].

BCI Summary

From the BCI state of the art, we retain that SVMs are a promising classification tool for the classification of neural signals relevant to the task at hand. Additionally, feature extraction methods which extract temporal information from specific time segments [38] are most relevant to the classification goal, particularly since it is applied to EEG data.

2.2.2 Epilepsy

Epilepsy is a disease that causes the brain to have seizures, decreasing the quality of life of a participant and can be life-threatening. Thus, methods of classifying [36], and even predicting [3], seizure activity is a largely developed field in Neuroscience.

Classification

Parvez et al. [36] successfully classified seizure EEG signals using least-squares SVM as an Ictal activity classification technique on features derived from DCT [36]. Bashar et al. were able to reach an accuracy of 0.792 in five subjects for epilepsy classification using a combination of features from the time-frequency domain [3].

Features

Ictal activity, which is a characteristic of epileptic brain activity, has a specific frequency imprint and thus can make locating it successfully if frequency features are used in classification. In an Ictal activity classification task, Parvez et al. [36] used DCT feature extraction for extracting the last 25% of DCT coefficients, which relate to high-frequency components as high Ictal signals are distinguished by the entropy and energy, which are derived from the high frequencies [36].

Epilepsy Summary

Overall, frequency extraction is an important feature to consider due to the nature of the epilepsy signal. Like selective attention, according to literature, it has much information to classify signals. This could be very applicable to selective attention data, as selective attention neural patterns tend to have a frequency band imprint as well [24], particularly in the N2PC region.

2.3 Machine learning for Attention

Neural Signal Classification, specifically for selective attention data, is considered quite a niche field. Thus, publications in the field are less common. Here are four selected application of classification to selective attention signals, for a clearer understanding of ML applications to attention selection datasets.

- 1 **LDA with N2PC signal amplitude: Fahrenfort et al [17]:** binary classification of target (intended object) selective attention using LDA with EEG signal amplitude as features.
- 2 **SVM with MEG signal amplitude: Wen et al [46]** binary classification of cue vs target object (distractor vs intended object) from MEG acquired selective attention data for Multivariate Pattern Analysis using SVMs with signal amplitude as features.
- 3 **LDA with N2PC signal amplitude: Moorselaar et al [32]:** Multivariate analysis to decode *location* of target vs distractor using LDA and signal amplitude features.

2.3.1 LDA with N2PC signal amplitude

In the study by Fahrenfort et al., participants were asked to answer if the color defined target (intended object) was a digit or a letter. Participants presented with a cue-target paradigm and classification were asked to determine if, from EEG signals alone, the classifier can distinguish if the stimuli were presented in the right vs. left of the screen, or top vs. the bottom of the screen (using LDA). The features used were signal amplitude (in microV) at each time instance. They trained an LDA, where the group's goal was to track feature-based target selection over time. Thus, they trained a classifier to classify, at each time sample, the presence of target selection neural activity. This was done by training one LDA classifier to learn if the target was on the right vs. left of the screen and one other LDA classifier to learn if the target was on the top vs. the bottom of the screen. Their classification resulted in a max accuracy score of 0.65.

2.3.2 SVM with MEG signal amplitude

Wen et al. applied Multivariate Pattern Analysis using SVMs to various binary classification tasks [46]. On average, classifier accuracy reached 0.65-0.67 accuracy, except for the stimulus identity classifier, which reached a 0.74 accuracy score. They classified overtime where at each time point, the feature was the amplitude

of MEG signal (much like Fahrenfort [17]). Additionally, their MEG analysis was able to classify selective attention earlier than the N2PC time-frame (used in EEG), suggesting that MEG might contain pre-N2PC attention selection information. Not as applicable as a result for the applications, but it is indeed interesting to see the suggested additional information MEG can extract.

2.3.3 LDA with N2PC signal amplitude

Moorselaar et al. [32] applied multivariate analysis to decode *location* of target vs. distractor using LDA and signal amplitude features. They trained an LDA classifier to discriminate between neural signals containing information regarding the target location for six different target locations, with a 0.26 percent accuracy score (Chance = 0.16).

2.3.4 Summary

For ML applications in attention selection datasets, no study directly parallels ours. However, there are similar studies with parallel approaches. From the four studies, LDA and SVM seem to be strong contestants for the classification of selective attention data. Additionally, the studies investigated time dynamics, meaning classification is applied at each time point, thus working with the amplitude of the signal rather than working with the frequency components.

2.4 Working Hypotheses

From the knowledge gathered about the Neuroscience and Machine Learning perspective of neural data and, more specifically, attention selection data, here are some working hypothesis:

- **Selective attention is separable in the frequency domain.** If selective attention has a distinct signature in the frequency domain (alpha and beta bands) [25], then selective attention is separable in the frequency domain.
- **N2PC regions hold most discriminative information.** If, as literature has shown, N2PC indicates presence of selective attention to both distractor objects [45, 15] and intended objects [7], then the N2PC region will hold more discriminative information than non-N2PC regions.

- **Non-specific regions *do* hold discriminative information.** If selective attention is a mechanism that requires various regions of the brain (as shown in Figure 1.4 [42]), then even non N2PC regions will hold information beneficial to the classification of selective attention EEG signals.
- **Baseline class (class 0) is separable from Distractor (class 1) and Intended (class 2) selective attention.** As the aim is to classify 3 types of attention - Distractor, Intended, or Baseline. Baseline class is a control class, with less selective attention markers than the other two attention classes. Thus, Baseline class should be most separable from Distractor and Intended. Additionally, Baseline should be less mistaken for one of the two true selective attention classes.

Chapter 3

Data, Methods, & Experimental Setup

This chapter elaborates on:

- 1 **Data:** The dataset used to achieve the desired goal.
- 2 **Methods:** The methods used for the analysis and experimental procedures.
- 3 **Experimental Setup:** The evaluation procedure applied to the experiments.

3.1 Data

The dataset consists of EEG-recorded neural activity of 39 adult participants. Dr. Turoman recruited the participants as part of her Ph.D. thesis [44]. To better understand how the dataset can answer the questions and support the hypothesis, a thorough explanation of the dataset and paradigm used in collecting the dataset is necessary.

3.1.1 Data: Paradigm

The paradigm is most similar to a previous study performed by Eimer et al [24], where the goal was to understand selective attention to *distractor object* known here as “Cue”. The paradigm also includes an *intended object* for selective attention known as “Target”. Additionally, there is a *baseline region* before distractor object onset, which is used as a baseline class for the goal of the thesis.

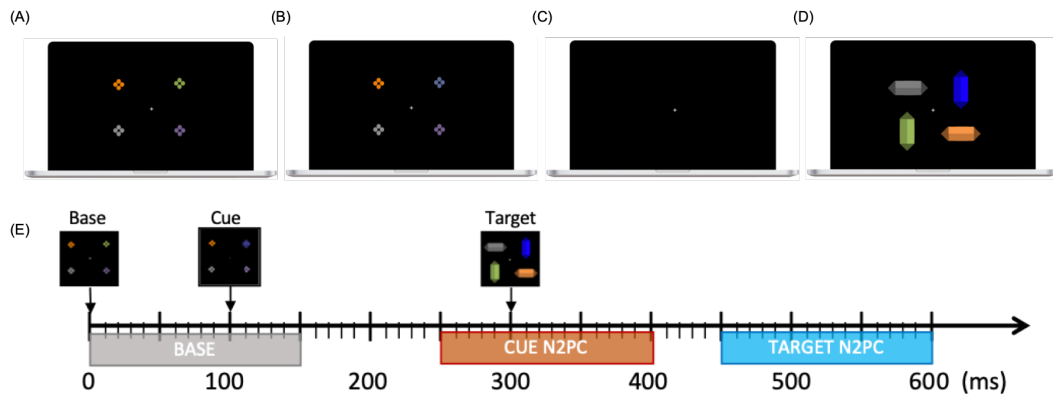


Figure 3.1: This figure shows all 4 stimuli of the paradigm (A - D) and the time importance of the three interested regions. (A) is “Baseline” Class 0, (B) is “Cue” Class 1, and (D) is “Target” Class 2 stimuli. The cross (C) is not used in this study. Additionally, (E) shows the temporal distribution of the N2PC components for the 3 selective attention stimuli (Distractor object = Cue, Intended object = Target, and no attention = Baseline).

In a similar setting to Figure 2.1, the participants are asked to perform a research study. The paradigm was designed to record many conditions (e.g., multiple senses and spatial cueing). However, this thesis focuses on the visual sense for visual selective attention, thus using only 1/4 of the dataset.

The participants took approximately 3 hours. The participants were instructed to search for a predefined color target (in this case, blue diamond) in a search array and report the intended object’s (blue diamond’s) orientation.

In this case, they were asked to report the orientation of a bar/diamond seen in Target image (Figure 3.1): to press a button on the left if the item was oriented horizontally, right button otherwise.

For example, in the sample image in Figure 3.1, the participant was asked to report the orientation of the **blue** bar at the beginning of the task. The participant would first see the base image (Baseline, class = 0), followed by the cue image (which has the **blue** color flower at the top right, but it is not a bar, thus deeming it a distractor object), then followed by the target image (which has the intended object at the top right) with the vertical blue shape. Therefore, a correct response would be to press the right button for the vertical blue bar. Each trial consisted of a base array (Baseline, class = 0), cue array (Cue, class = 1), then target array (Target, class = 2). The timing of each array is shown in Figure 3.1 with the relevant N2PC regions of interest for extraction (Distractor object = Cue, Intended object = Target, and neither = Baseline). In other terms, the goal of this thesis is to classify Baseline, Cue, and Target objects from EEG data collected with Turoman’s paradigm, in a fast, objective manner.

3.1.2 Data: Acquisition

The EEG dataset was collected using a 129-channel HydroCel Geodesic Sensor Net connected to a NetStation amplifier (Net Amps 400; Electrical Geodesics Inc., Eugene, OR, USA) where 128 electrodes were used at 1000 Hz sampling rate. During data acquisition, electrode impedances were kept below $50k\omega$, and electrodes were referenced online to Cz, a common reference for EEG cap data collection. Participants were recorded for 3 hours in a task described in Turoman et al. [45]. This dataset was collected by Dr. Turoman during her Ph.D. work [44].

3.2 Methods

3.2.1 Preprocessing

The preprocessing is based on state-of-the-art works [44, 15, 24]. To parallel other studies for selective attention, relevant procedures for preprocessing the attention acquired from EEG were performed. To get an overview of the complete preprocessing procedure, see Figure 3.2.

Preprocessing: Cartool

Post extraction, the first phase of preprocessing was applied using Cartool software [2]. In respective order, data were band-pass filtered between 0.1 Hz and 40 Hz, notch filtered at 50 Hz, and Butter-Worth filtered of phase shift elimination at -12 dB/octave roll-off. Automatic artifact rejection of +/- 100 micro-Volts was used to increase the signal to noise ratio. Next, trials were segmented to include base, cue, and target array neural responses, respecting the time range in Figure 3.1. The data was further inspected for bad electrodes and screened for noise, eye movement, and muscle artifacts resulting in the rejection of 11% of trials across all participants in the dataset. This preprocessing procedure has been replicated as per Turoman et al. [45]. See Figure 3.2, A-1 to A-3, for the preprocessing illustrated flowchart.

Preprocessing: Global Field Power (GFP) Normalization

To make the EEG data independent of amplitude strength across all electrodes at each time point, Global Field Power (GFP) normalization is applied to all datasets. At each time sample, each electrode value is divided by its standard deviation. GFP normalization was performed in B-1 (Figure 3.2). Global field power is a measure of amplitude strength at a certain point across all electrodes. Mathematically, GFP

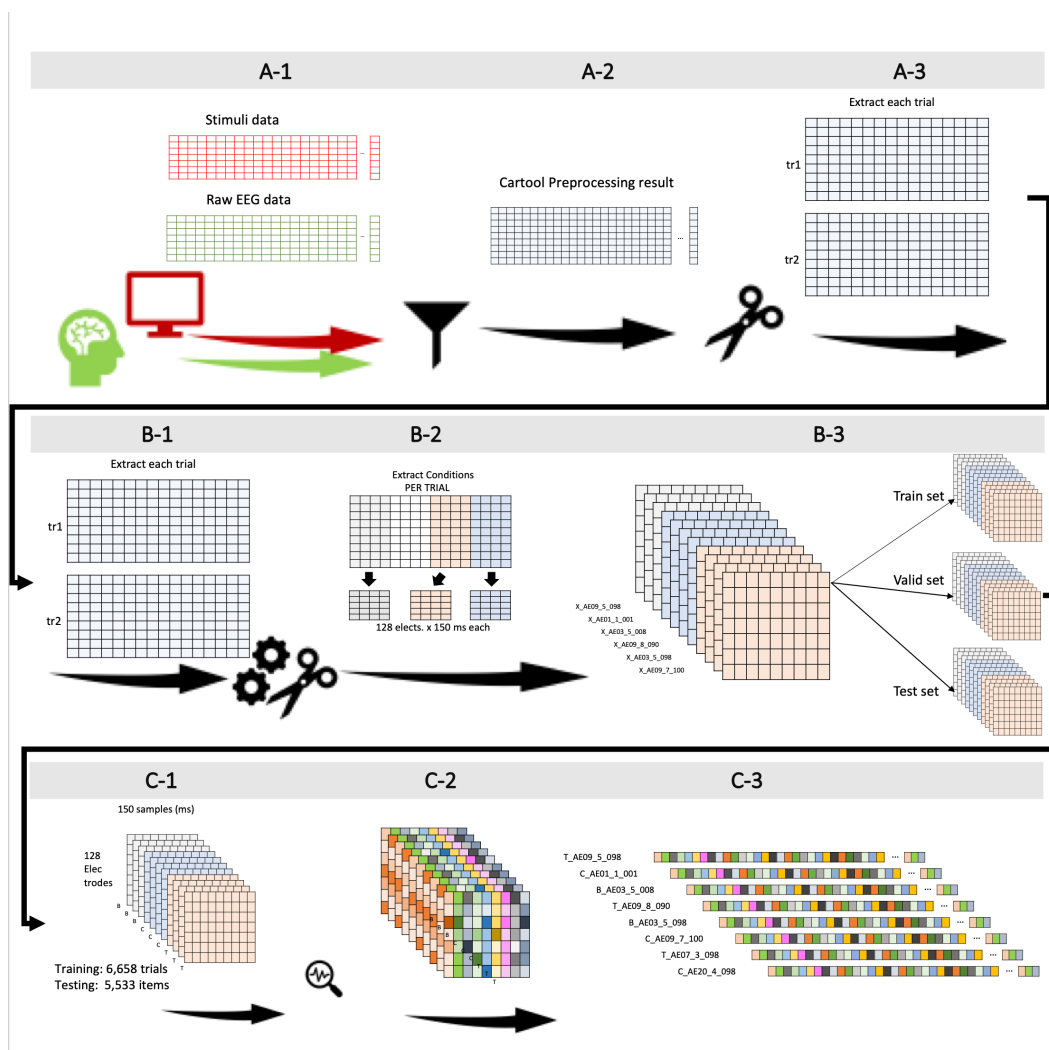


Figure 3.2: **Overview of the complete preprocessing procedure**, from data acquisition to feature vector formation. (A) is the preprocessing performed in Cartool [2], (B) is further preprocessing and restructuring of the dataset for the purpose of the projects goals see, and (C) is the feature extraction with DCT).

is the root mean square across the average referenced electrode values x at a given time sample i (see Equation 3.1), i.e., the standard deviation of all the electrodes at that point in time. For ERP's, this equals the potential across all electrodes, and it is a measure of potential as a function of time or time-samples.

$$GFP_x = \sqrt{\frac{\sum_{i=1}^n x_i^2}{n}} \quad (3.1)$$

Preprocessing: Dataset Split

The dataset was segmented into the base, cue, and target time-regions, each of length 150ms (at 1000 Hz, this equals 150 samples each). Then, each segmentation was labeled as 0 or “B” for the Baseline, 1 or “C” for the Cue, and 2 or “T” for the Target, with additional information being stored with the label, such as participant code, block number, and trial number. The total trials used across participants is 4063 for each class.

To ensure the generalizability of the thesis' experiments, the dataset was split by participants into Train, Validation, and Test sets. The ratio of the split was 40 - 20 - 40 %, respectively. See Figure 3.3, A) - C) for a more visual description of the organization and structuring of the dataset.

3.2.2 Feature Extraction

In ML, feature extraction is the process of extracting information from a signal that best represents the unique features of said object/image/signal. One method for frequency feature extraction is the Discrete Cosine Transform (DCT) [14]. DCT is a transform of any signal (image or time series) into basic frequency components of size = signal length – 1.

Discrete Cosine Transform (DCT)

DCT is generally used as a compression mode with very low loss of images and, more recently, used in speech processing in cepstral feature analysis. Equation 3.2 one dimensional DCT, relevant to the thesis. Additionally, DCT can also be used as a feature extraction method to extract frequency components of a signal [22, 36], particularly for EEG and MEG data acquisition methods.

$$y_k = 2 \sum_{n=0}^{N-1} x_n \cos\left(\frac{\pi k(2n+1)}{2N}\right) \quad (3.2)$$

For a 150 sample long signal sampled at 1000Hz, the data's features included frequencies from 0 to 500 Hz, linearly contained within 149 DCT bins for each electrode. Prior knowledge of attentional frequency oscillation dictates that selective attention ranges from 8 Hz to 30 Hz (alpha and beta ranges)[24]. For the data's DCT extraction, this range is contained in DCT bins 2 to 10. Thus, the smaller DCT bins will likely contain more relevant information to selective attention than others.

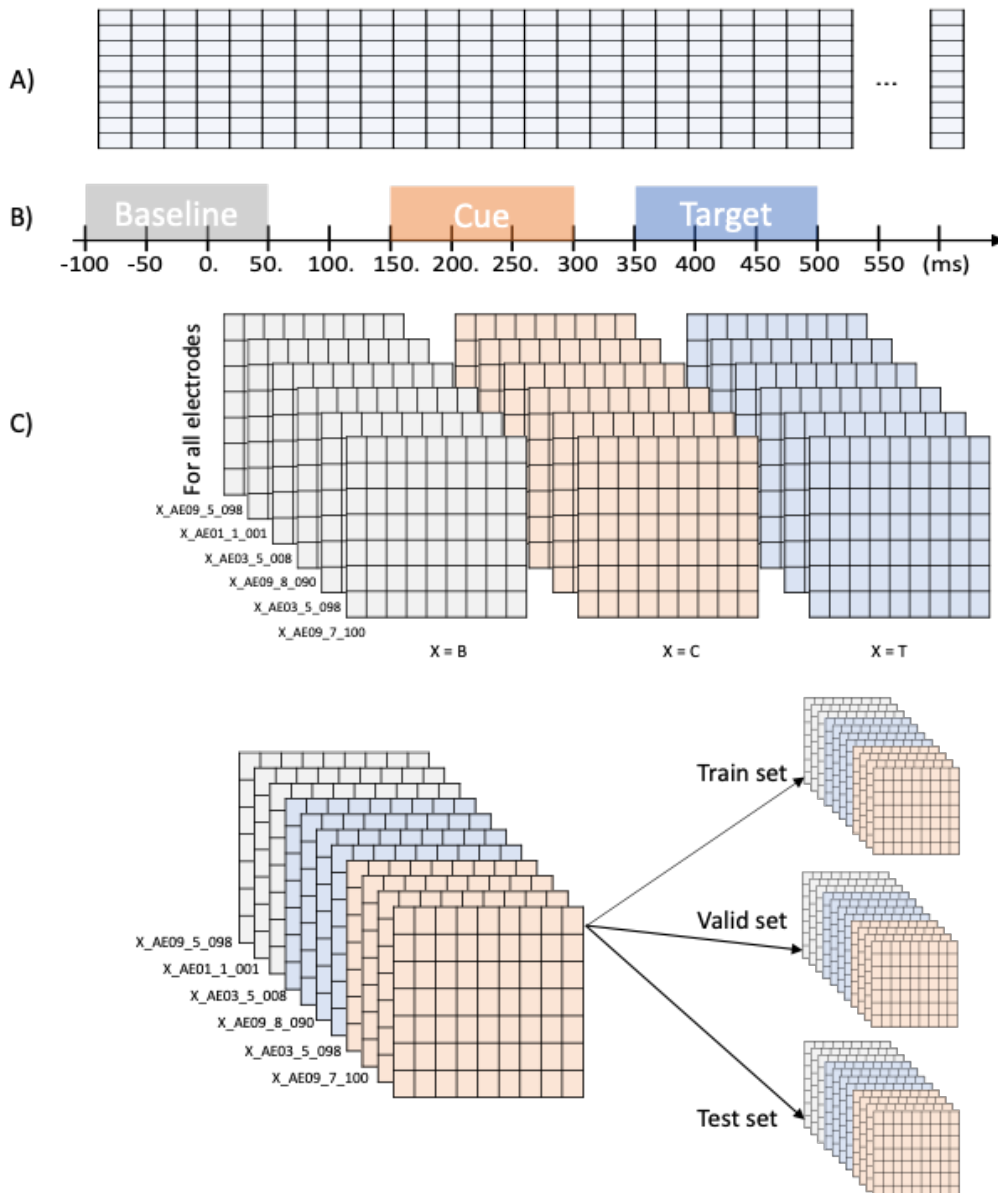


Figure 3.3: Using Cartool software, the standard EEG preprocessing is applied, followed by extracting EEG data of interest. (A) whole experiment, (B) time intervals of interest (Baseline, Cue, and Target) within each trial, for each participant, and (C) splitting each trial (of 600 ms) into 3 data samples (150 ms each) with appropriate labels (Baseline, Cue, Target), then reordering and splitting into train, test, and validation sets. (Distractor object = Cue, Intended object = Target, and neither = Baseline).

Among the many feature extraction methods for EEG data[28, 29], DCT feature extraction was most logical to eliminate temporal and amplitude information, as the hypothesis states that frequency components will hold the most separable information during the classification of the three classes. DCT feature extraction steps are visualized in Figure 3.2, C-1 to C-3, which is applied to all datasets (Train, Validation, and Test). During DCT extraction, an EEG signal of size 128 electrodes times 150 time samples is transformed into a signal of 128 electrodes times 150

DCT bins. The first DCT bin, i.e. the DC component, is discarded to result in a feature matrix of size 128 electrodes times 150 DCT *frequency* bins (Figure 3.2, C-1 to C-2). Then, the matrix is restructured to create a 1D feature vector of size 19072 (128*149) features. The restructuring is performed so that, as the indexing increases, so does the frequency component.

Prior knowledge of attentional frequency oscillation dictates that selective attention ranges from 8 Hz to 30 Hz, with higher importance in the 8-12 range (alpha oscillations) [25]. The DCT bins hold information from 0 Hz to 500 Hz. Thus, it is likely that the initial DCT bins will hold more separable information.

3.2.3 Data Visualization

The goal of data visualization for preprocessed data is to verify and take note if the data is behaving as we expect it to. If the visualized data is within expected values, the preprocessing stage starts. If not, the data is tagged for further preprocessing or is removed from the dataset. This is the nature of many cortical activity measurements, and it requires a trained eye to “classify” which electrodes are proper and improper. For example: To interpolate the bad electrodes in the EEG dataset, visualizing the data is necessary. This way, many anomalies can be detected, including 50Hz noise and bad electrodes that require interpolation.

Data Visualization: Preprocessing

Figure 3.4 reflects the differences in EEG signal preprocessing (for one trial), from stage A-1 to stage B-3 of Figure 3.2. In other words, the result of preprocessing from EEG data acquisition until separating. It is important to note the removed bad electrodes (in gray), which are interpolated for not losing data. All results are plotted using the MNE toolbox [31].

Data Visualization: Feature extraction

As mentioned, the selected method for feature extraction is DCT applied to each electrode. This process is a continuation of the preprocessing steps mentioned in Figure 3.2 (steps C1 - C3). The electrode matrix of size 128 x 150 was transformed using DCT resulting in a well-formulated feature vector of 128 electrodes and 150 DCT components. Since only the frequency components of the DCT were of interest, we removed the first DC component, resulting in a final feature vector of 128 x 149 frequency bins for a length of 19072 features per sample.

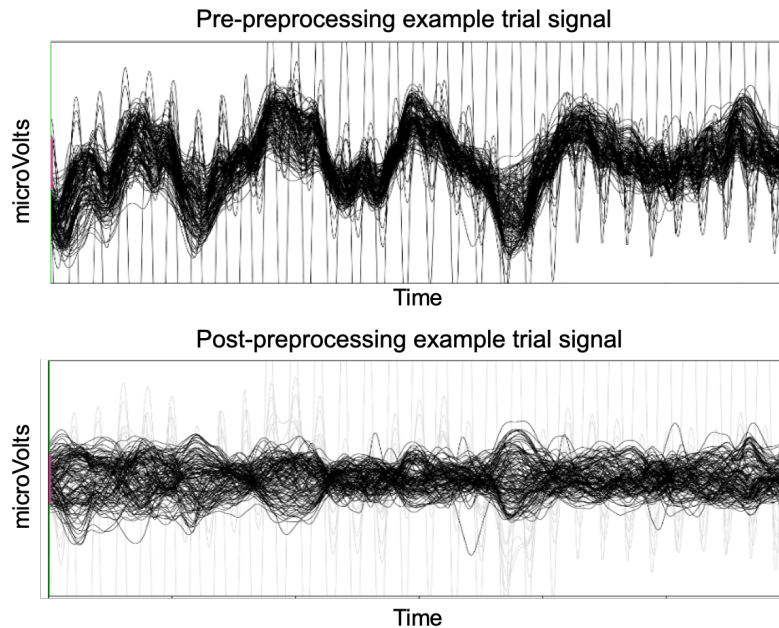


Figure 3.4: **Acquired EEG data vs last stage of preprocessing, results**, visualized with MNE [31]. The plot shows all EEG electrodes (128) for one trial of the experimental acquisition, in butterfly view (all electrodes centered at 0 microV). Difference between the figures is a result of (i) removing bad electrodes (gray signals), (ii) interpolation and (iii) filtering for 50 Hz noise.

3.2.4 Dimensionality Reduction

Dimensionality reduction was performed on the dataset. The aim of dimensionality reduction was to decrease the amount of features needed for the classifier to learn and perform well. The two most common techniques used were PCA and LDA.

Dimensionality reduction: PCA

PCA looks for a direction that keeps most of the variability of the data. PCA is a method that finds the projection which maximizes the variability of the dataset and how much of the variability is explained. PCA is a very popular technique used for dimensionality reduction in an unsupervised manner. However, PCA is not necessarily the most applicable for EEG and brain processes in general due to the low signal-to-noise ratio of EEG signals. Artoni et al. applied PCA to EEG data for source separation and found that PCA rank reduction reduced the number of participants represented in independent component clusters and increased uncertainty in the independent component brain sources [1]. Through this, PCA minimizes reconstruction loss.

Additionally, PCA assumes that variance is equal to the relevance of a signal. EEG datasets, which have a lower signal to noise ratio than other more invasive cortex

activity measures, include muscle artifact activity, electrical and mechanical noise, with much more covariance than the desired source (i.e., attention mechanisms). Nonetheless, if handled properly, PCA is good for reducing the dataset from M to C dimensions where $1 < C < M$.

Dimensionality reduction: LDA

For datasets where dimensionality reduction is used to separate the dependent variable by preserving their differences, Linear Discriminant Analysis (LDA) is helpful [9]. LDA finds a low-dimensional projection of n groups or classes so that they are well separated. LDA identifies an ordered set of $n - 1$ directions that best maximize the variance between the n groups or classes. As such, LDA's ability to separate n classes of training data improves as the data dimensionality increases. Of course, increasing the dimensionality of the dataset can be troubling as with a high enough dimensionality, any fixed number of data points can be separated at one arbitrary dimension. Hence, LDA use requires caution and regularization when dealing with very high dimensionality but low training datasets [29].

Dimensionality reduction: Manual

One downfall of dimensionality reduction algorithms is that they assume there is no structure associated with each dimension. In fact, there are a plethora of structures associated with each concurrently active process explained in the state of the art. For example, attention requires vision, task-set feature selection, motor planning, all processes that are concurrently active and difficult, but not impossible, to extract from LDA or PCA. With careful consideration and proper feature use, this is suggested to be possible in BCI [29] classification, Ictal activity prediction and classification [3], and selective attention classification [17, 32].

Nonetheless, we applied manual dimensionality reduction based on the knowledge of the state of the art. In selective attention, certain frequency bands and certain electrodes should have higher discriminating power than others.

3.2.5 Dataset Normalization

In case the datasets are giving errors or the model scores are not consistent, whether in the accuracy score or the confusion matrices values, it is beneficial to perform simple dataset analysis techniques that test:

- 1 Class balance.** Counting all classes have a similar amount of representation. For the paradigm, the classes are perfectly balanced, as there are as many Baseline samples and Target or Cue.

2 Normalization values. The dataset has been feature scaled, which is a method that brings all values of the feature vector into the range of [0,1]. Feature scaling is performed using the mean and standard deviation of the Training set. To check how well the normalization is applied to the Validation and Test sets, the mean and standard deviation values are visualized, in case they range significantly larger than [0,1]. This can be an indication of heterogeneity in the dataset.

3.2.6 Classification

Two main classification algorithms have been used, Logistic Regression (LR) [27] and Support Vector Machines (SVM) [43], implemented using the scikit-learn library freely available on Python [40].

Classification: LR

Logistic regression is used as a categorical problem solving [27]. It can be applied to multivariate classification. It is deemed a simpler classification technique but can provide unique results if feature vectors are adequately selected and if the data is linearly separable.

For preliminary testing, in an attempt to prove the hypothesis by using a simple to implement and easy to interpret model, a Logistic Regression classifier was trained.

Classification: SVM

Pavrez et al. successfully classified seizure EEG signals using least-squares SVM as an Ictal activity classification technique on features derived from DCT, EMD, or both [36]. As a non-linear option classifier, SVM classification (SVM) was used in this thesis, as well. SVM classification attempts to find the hyper-plane that separates the dataset the best. For non-linear datasets, a general "RBF (Radial Basis Function)" kernel is used.

Classification: Application

Following the general Supervised classification procedure (see Figure 1.5), supervised classification is employed to classify types of attention signals (Baseline, Cue, and Target). To discriminate the type of attention, the features are frequency components extracted from DCT, and the labels associating with the feature vectors

are Baseline, Cue, or Target (otherwise, Neither attention, Distractor attention, or Intended object attention).

The chosen classifier is trained to classify the neural information into one of the labels. Thus, when new, unlabeled information is presented, the model can *predict* which label the neural information most likely belongs to.

3.3 Experimental Setup

In this section, I introduce the Evaluation method applied to test the four working hypotheses. To have a good flow of analysis, I replicate the structuring of the experimental setup section to the Experimental Results chapter and the Discussions chapter.

3.3.1 E1: Classifying frequency domain features

To test the hypothesis that selective attention is separable in the frequency domain, two experiments have been organized. The two experiments use different sets of DCT bins. Post DCT feature extraction of the EEG dataset (the result of following the preprocessing procedure explained in figure 3.2), the experiments are as follows:

E1.a: Compare classification of DCT[1,49] to DCT[50,99] and DCT[100,149]

As attention has an alpha-beta frequency range [24], DCT components in that range should hold higher separability information. Alpha-beta frequencies are encoded in the first 50 DCT bins. Thus, the first experiment was to attempt to classify selective attention in the range of:

- 1 to 49 DCTs
- 50 to 99 DCTs
- 100 to 149 DCTs

This classification was replicated in the above 3 conditions using LR for a linear classifier and SVM for a non-linear classifier. The parameters of each classifier, using *sklearn* library [27, 43] are as follows:

- LR: C = 0.001, fit intercept = False, multi class = 'ovr', solver = 'newton-cg'

- SVM: kernel='RBF', decision function shape = 'ovr'

If the results of the LR and SVM classifiers show that for ranges of 1 to 49 DCTs the performance accuracy was higher than for the other ranges (50 to 99 or 100 to 149), then we do not reject the hypothesis that selective attention is separable in the frequency domain.

E1.b: Compare classification of DCT[1,49] to DCT[1,99] and DCT[1,149]

Additionally, the classification with the above mentioned LR and SVM was replicated for DCTs from 1 to 99 and DCTs 1 to 149, to compare the performance accuracies of the alpha-beta frequency features to the use of more (1 to 99) and all (1 to 149) DCTs:

- 1 to 49 DCTs
- 1 to 99 DCTs
- 1 to 149 DCTs

Additionally, if the performance of the LR and SVM classifiers was lower for DCTs of 1 to 49 when compared to using 1 to 99 DCTs or 1 to 149 DCTs, we do not reject the hypothesis that selective attention is separable in the frequency domain.

In order to more strongly reject or not reject the hypothesis, cross validation techniques are applied to validate the results.

For this, GridSearchCV [8] from the Python library *sklearn* was utilized. Depending on the performance accuracy of SVM and LR classifications, cross-validation using GridSearchCV seemed similar, it was important to apply fine-tuning via cross-validation techniques using *sklearn*'s GridSearchCV library on three highest accuracy performances DCT ranges. The parameters that were cross-validated were C and γ for SVM and C and $max\ iterations$ for LR. The cross-validation was 10 fold. Only optimized results of the GridSearchCV were reported to help reject or not reject the hypothesis that selective attention is separable in the frequency domain. The highest performance accuracy score and the average performance accuracy score were compared with other experimental results.

3.3.2 E2: Classifying N2PC and non-N2PC Region features

To test the hypothesis that selective attention is likely more separable in the N2PC regions, a set of sub-experiments have been organized. The *E2* experiment parallel *E1* experiment, with the difference that N2PC and non-N2PC region electrodes be selected instead of DCT frequency features. These N2PC and non-N2PC regions are visualized in Figure 3.5.

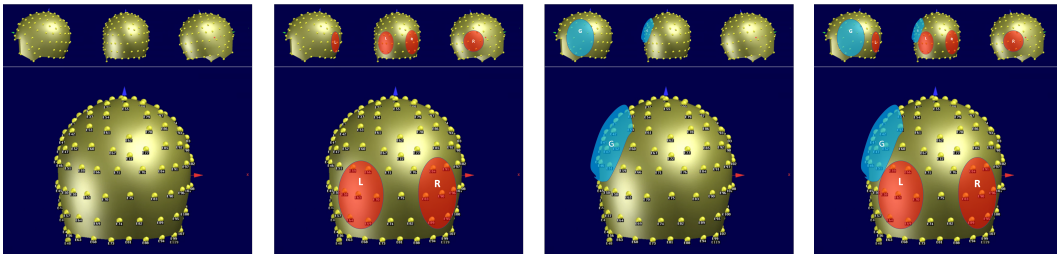


Figure 3.5: **EEG Cap images** showing the regions of interest (from left to right) of a full electrode coverage, N2PC regions (E2.a Electrodes) in red, non-N2PC regions (E2.b Electrodes) in blue, and the lack of overlap between N2PC and non-N2PC regions.

E2.a: Classifying N2PC electrodes

For this experiment, in order to reject or not reject the hypothesis that (H2) selective attention is separable in N2PC regions, only features from N2PC regions electrodes were used. In literature, it is highly accepted that N2PC is a marker for selective attention [45, 16, 24, 33]. In traditional N2PC analysis of EEG data, the posterior-contralateral electrodes and the surrounding neighbouring electrodes are used, and LR and SVM classification is applied. The parameters of the classifiers are the same as *E1*. Electrode selection for the N2PC region includes:

E2.a Electrodes = [e65 e90 e58 e96 e59 e91 e64 e95 e66 e84 e69 e89 e70 e83]

Additionally, much like in experiment *E1*, cross-validation using GridSearchCV is applied for *E2.a*.

E2.b: Classifying non-N2PC electrodes

Although N2PC is a marker of selective attention, non-N2PC regions can still have discriminating information about attentional selection, as attention has a *whole brain* activity presence. To reject or not reject the hypothesis that (H3) non-N2PC regions contain discriminative information on classifying selective attention, only features from non-N2PC regions electrodes were used. This included using the following non-N2PC electrodes:

E2.b Electrodes = [e35 e36 e37 e38 e39 e40 e41 e42 e43 e44 e45 e46 e47 e48]

To help visualize the selected N2PC and non-N2PC regions, see Figure 3.5. Additionally, similarly to experiment *E1* and as in standard ML approaches, hyperparameter optimization and cross-validation using GridSearchCV are applied for *E2.b*.

3.3.3 E3: Identify which class is the most separable

The goal of this experiment is to test the hypothesis that classes related to selective attention (such as Cue and Target classes) are separable from the control condition (Baseline). As the Baseline should not have selective attention activity encoded in the features, the Baseline class should be most separable from Distractor and Intended classes. In order to reject or not reject this hypothesis, confusion matrices will be computed and weight coefficients and prediction probabilities will be analyzed.

E3.a: Compute Confusion Matrices of learned classification models

Confusion matrices are calculated to portray the classification accuracy scored of each class in mean and standard deviation over a 10-fold cross-validation using GridSearchCV [8]. Jointly, the ten performance accuracies associated with those confusion matrices (also with mean and standard deviation) are reported.

The aim of calculating the confusion matrices of the learned models is to better understand errors the learned model is making, particularly in the class performance. To not reject the hypothesis that (H4), Cue and Target classes are separable from the Baseline class, the errors within Baseline-Cue and Baseline-Target need to be smaller than the errors within Cue-Target. To do so, the confusion matrices are plotted. This is applied to both LR and SVM for top-performing DCT frequency ranges and N2PC regions.

E3.b: Analyse weight coefficients of learned models

To reject or not reject the hypothesis that (H4) Baseline class is more separable than Cue and Target, analysis on the weight coefficients of each learned classifier (Baseline, Cue, Target) are plotted in order of DCT features and also in order of electrodes. The purpose of this is to facilitate the view of patterns/analysis of the resulting weight coefficient. If a pattern emerges, where some features are consistently of high weight for a class, then it is likely that that feature highly influences the decision of the classifier. If there is no such pattern seen, particularly between attention (Cue and Target) compared to non-attention (Baseline), H4 is rejected.

E3.c: Analyse prediction probability of learned classifiers

To reject or not reject the hypothesis that (H4) Baseline class is more separable than Cue and Target, analysis on the classifiers prediction probability are done. For this, the trained LR model is used in the *ovr* setting. The expected results

of this experiment are to predict the probability (values between 0 and 1) of the validation set using each classifier within the model. Then, plot the calculated probability of each class (Baseline, Cue, Target).

To not reject hypothesis H4, errors in prediction probability of the true Baseline label should be lowest of the 3 labels in the Cue and Target classifiers. If either Cue or Target classifier prediction probabilities frequencies are higher at 1 for Baseline than for the other, H4 is rejected.

3.3.4 E4: Dimensionality Reduction to strengthen decisions to reject or not reject hypotheses

To reject or not reject the four hypotheses and to reach the overall aim of classifying selective attention, this thesis follows a (i) simple and easy approach at first, then a (ii) more complex approach, followed by possible (iii) dimensionality reduction techniques. Dimensionality reduction was applied to the dataset to decrease the dimensionality of the feature vector, as the size of the feature vector was quite large, given the limited number of samples. The goal of dimensionality reduction is to further strengthen the confidence in the concluded decision-making. Dimensionality reduction results are evaluated by performance accuracy on the test set.

Two dimensionality reduction approaches used in this thesis are PCA[41] and LDA[26], both from the *sklearn* library, freely available in Python.

E4.a: LDA

To reduce the number of features, LDA is a preferred technique for attention data [17, 32]. LDA was applied to the dataset with all DCT and electrode features. Post LDA transform, LR classification was applied to the LDA transformed dataset, and a performance accuracy was reported. The before and after LDA transformed LR performance accuracies were noted. Additionally, confusion matrices were reported.

E4.b: PCA

For the similar reason as LDA, PCA was used to attempt to reduce the size of the feature vector. Thus, reducing the dimension of the feature vector. PCA was applied to the dataset with all DCT and electrode features. PCA was applied to contain:

- .50 of variance
- .70 of variance
- .90 of variance
- .95 of variance
- .99 of variance

LR classification was applied to the transformed dataset, and a performance accuracy was reported. The performance accuracy scores post-PCA was compared to the average accuracy score of LR with optimized hyper-parameters.

Chapter 4

Experimental Results

All experiments described in this chapter are to reject or not reject our working hypothesis. To facilitate the flow of information, this chapter is divided into four sections reflecting the four working hypothesis formed in the last section of Chapter 2.

In summary, the 4 hypothesis are as follows:

- H1** If selective attention has a distinct signature in the frequency domain (alpha and beta bands) [24], then selective attention is separable in the frequency domain.
- H2** If N2PC indicates presence of selective attention to both distractor objects [45, 15] and intended objects [7], then selective attention is separable in the N2PC region features.
- H3** If selective attention is a mechanism that requires various regions of the brain (Figure 1.4 [42]), Non-specific regions *do* hold discriminative information.
- H4** If Baseline does not hold any selective attention information, then Baseline (class 0) is separable from Distractor (class 1) and Intended (class 2) selective attention

4.0.1 R1: Classifying frequency domain features

R1.a: Compare classification of DCT[1,49] to DCT[50,99] and DCT[100,149]

The first experiment is to attempt to classify selective attention in the DCT ranges specified in the experimental setup. This was done in both LR and SVM classification methods. The parameters of each classifier, using *sklearn* library [27, 43] are

[C = 0.001, fit intercept = False, multi class = 'ovr', solver = 'newton-cg'] for LR and [kernel='RBF', decision function shape = 'ovr'] for SVM. The resulting performance accuracies of these classifiers are shown in Figure 4.1.

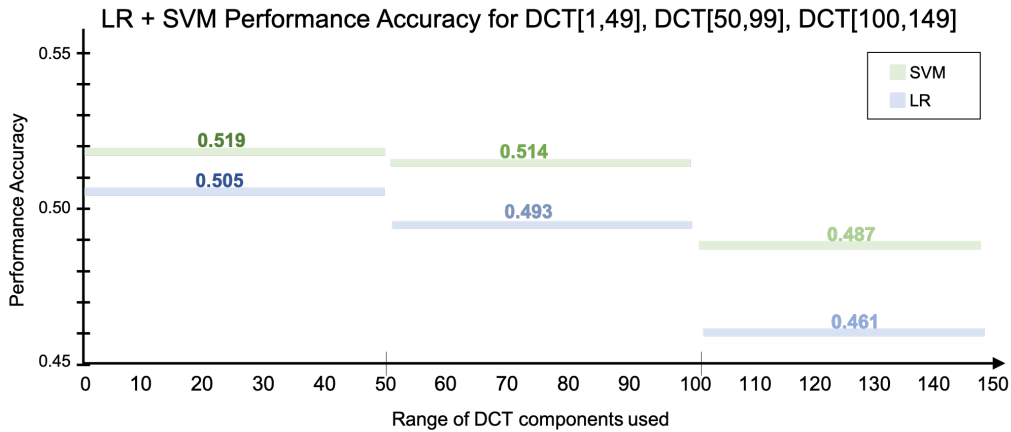


Figure 4.1: **Classification of DCT[1,49], DCT[50,99] and DCT[100,149] using LR and SVM classifiers.** The *average* performance accuracy from the 10 fold cross-validation is plotted for each DCT component range. LR in blue, SVM in green.

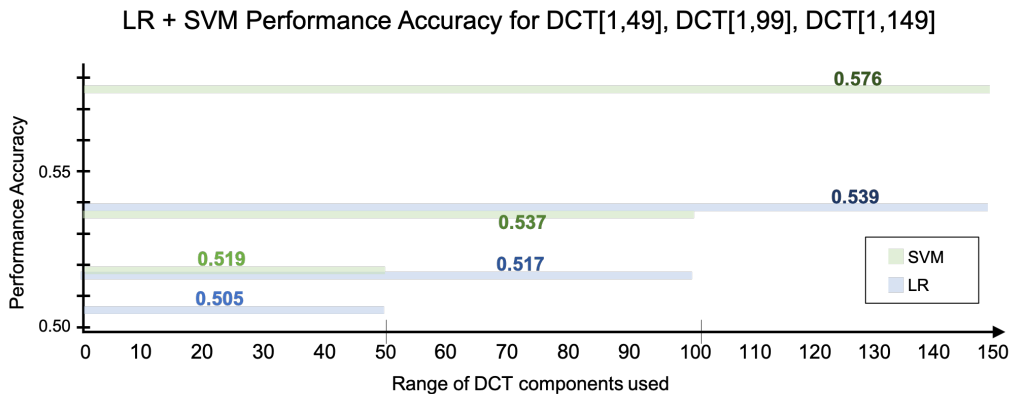


Figure 4.2: **Classification of DCT:** LR and SVM classification results as *average* performance accuracies from the 10 fold cross-validation for DCT[1,49] to DCT[1,99] and DCT[1,149]. LR in blue, SVM in green. The *maximum* performance accuracies for [LR,SVM] are [0.60,0.60], [0.61,0.62], [0.65,0.65] for DCT[1,49] to DCT[1,99] and DCT[1,149], respectively.

R1.b: Compare classification of DCT[1,49] to DCT[1,99] and DCT[1,149]

As this experiment is similar in setup as the previous one, the explanation is the same. Average performance accuracies across the 10 fold cross-validation were performed in three groups of DCT components. The only difference is the range of DCTs used. Instead of DCT[1,49] to DCT[50,99] and DCT[100,149], this sub-experiment classified DCT[1,49] to DCT[1,99] and DCT[1,149]. These results are plotted in Figure 4.2. Additionally, *maximum* performance accuracies

for [LR,SVM] were recorded, for later comparison. For [LR, SVM]: [0.60,0.60], [0.61,0.62], [0.65,0.65] for DCT[1,49] to DCT[1,99] and DCT[1,149], respectively.

For the 10 fold cross validation, an LR classifier was retrained in 10 unique data splits. When using all features, both LR and SVM resulted in a performance accuracy score of 0.59 on average and 0.65 for the best-case scenario. This is shown in the first plot of Figure 4.3. Both LR and SVM classification performed similarly (average 0.59, best 0.65 accuracy scores).

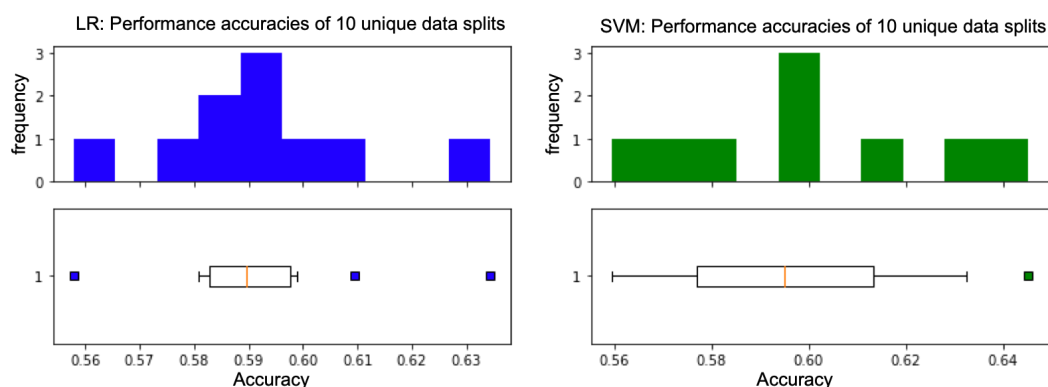


Figure 4.3: Performance (accuracy scores) of LR and SVM over 10-fold cross validation.

To make the results generalizable to other new participants, The data-splitting was initially performed per-patient. In turn, the participant data was split into train validation, and test sets. Additionally, the training set was used to fit the model, the validation set for hyper-parameter optimization and general tuning, and the test set was used to result in the performance accuracy of the classifier. Both an LR and SVM classifier was used for this experiment. The results for the ten performance accuracies are shown in Figure 4.3.

For SVM, in addition to the average mean and standard deviations histogram and box-plot or performance accuracy, the confusion matrices were reported. The confusion matrices portraying the classification accuracy scored of each class, in mean and standard deviation. The performance accuracy results are shown in plot 2 of Figure 4.3, and the confusion matrix is shown in Figure 4.6, right side.

Mean and standard deviation of the train, validation, and test sets were computed, to check if normalization was applied appropriately. The resulting plots of the mean and standard deviation are shown in Figure 4.4.

The top graph shows the mean (at $x = 0$) and standard deviation ($x = 1$ range) of the Train (black/grey), validation (red/pink), and test (light blue/blue) datasets. The bottom three graphs are for each Train Validation and Test set, showing the distribution of features in each class; Baseline (gray), Cue (red), and Target (Blue).

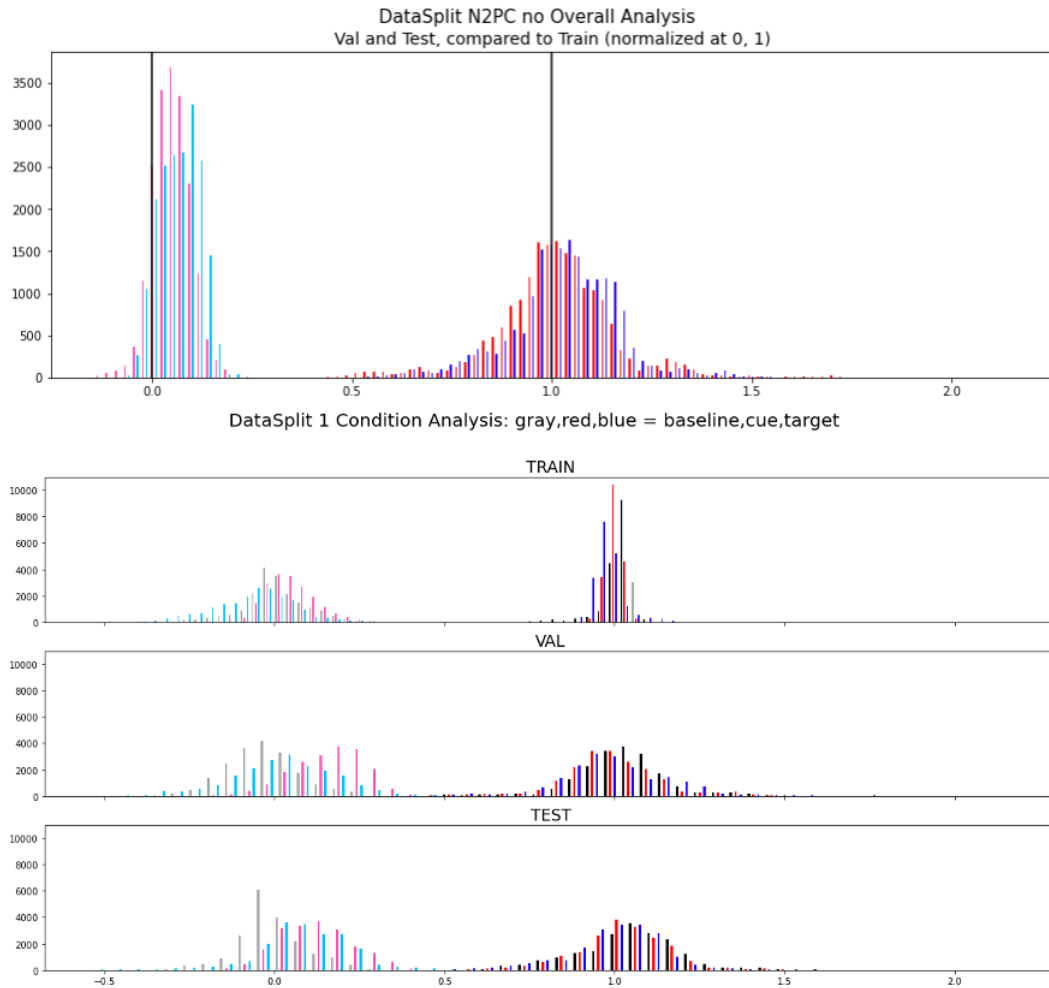


Figure 4.4: Figure showing (mean,standard deviation) of the training set, validation set and test sets. The top graph shows the mean (at $x = 0$) and standard deviation ($x = 1$ range) of the Train (black/grey), validation (red/pink), and test (light blue/blue) datasets. The bottom three graphs are for each Train Validation and Test set, showing the distribution of features in each class; Baseline (gray), Cue (red), and Target (Blue).

4.0.2 R2: Classifying N2PC and non-N2PC Region features

The summary of the results of *average* classification performance accuracy for all electrodes, N2PC features, and non-N2PC features are shown in Figure 4.5. This figure includes the resulting performance accuracies of the 10-fold cross-validation, and the confusion matrices of the ten fold learning, with mean and standard deviation values. Additionally, *maximum* performance accuracies for [LR,SVM] were recorded. For [LR, SVM]: [0.65,0.65], [0.61,0.65], [0.52, 0.53] for all electrodes, N2PC electrodes, and non-N2PC electrodes, respectively. All DCT features were used for this analysis (DCT 1-149).

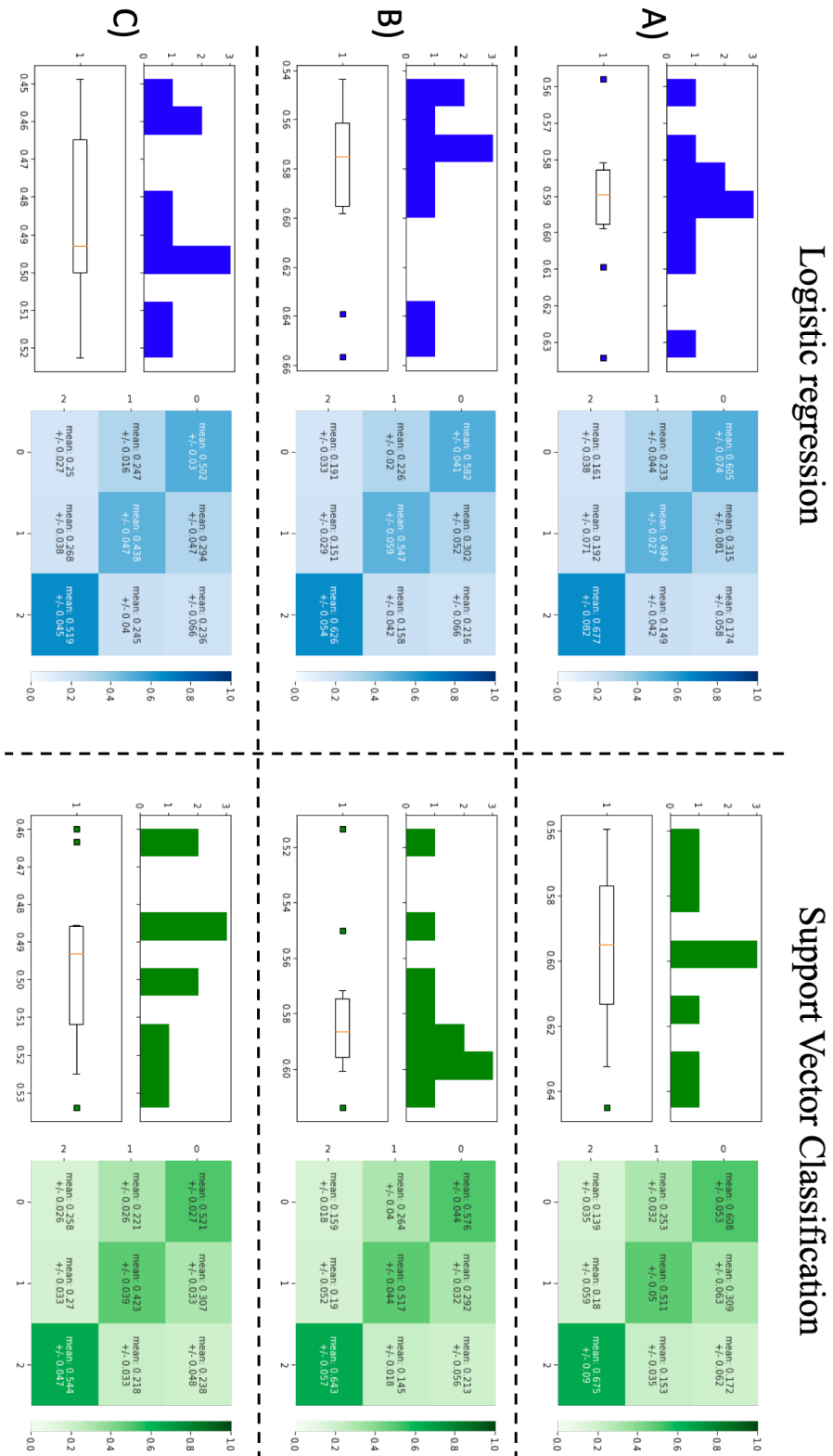


Figure 4.5: Classification Accuracy scores between LR and SVM on (A) all electrodes, (B) N2PC electrodes, (C) and non-N2PC electrodes, for Baseline = 0, Cue = 1, and Target = 2.

R2.a and R2.b: Classifying N2PC electrodes and non-N2PC electrodes

The resulting performance accuracies for the non-N2PC feature classification are reported in Table 4.1 . Additionally, Table 4.1 shows a numerical summary of the graphs in Figure 4.5, which includes all features, N2PC features vs. non-N2PC features *average* performance accuracies between LR and SVM and related confusion matrices.

		Logistic Regression Accuracy	Support Vector Classification Accuracy
		$\mu_{Accuracy} \pm \sigma_{Accuracy}$	$\mu_{Accuracy} \pm \sigma_{Accuracy}$
All Electrodes	Full coverage 128 electrodes	0.5920 ± 0.0190	0.5992 ± 0.0261
Selected Electrodes	N2PC region 14 electrodes	0.5850 ± 0.0352	0.5797 ± 0.0275
	Non N2PC region 14 electrodes	0.4865 ± 0.0234	0.4956 ± 0.0230

Table 4.1: Table of *Average* Classification Accuracy scores for the 10 fold cross-validation between LR and SVM on (i) all electrodes, (ii) N2PC electrodes, and (iii) non-N2PC electrodes

4.0.3 R3: Identify which class is the most separable

R3.a: Compute Confusion Matrices of learned classification models

Confusion matrices were calculated to better understand errors the learned model was making, particularly in the within class performance. Confusion matrices were calculated for (i) N2PC vs non-N2PC feature comparisons (Figure 4.5, (ii) comparing SVM and LR performances (Figure 4.6) , and (iii) Dimensionality reduction for PCA and LDA (Figure 4.10 and Figure 4.9, respectively).

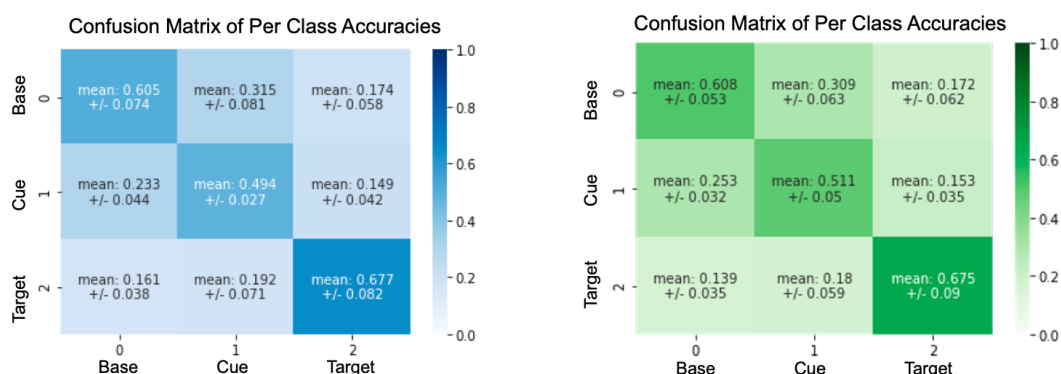


Figure 4.6: Confusion Matrices of LR and SVM over 10 fold cross validation. The accuracy scores are shown for each class true labels (y axis) and predicted labels (x axis), for Baseline (Class 0), Cue (Class 1), and Target (Class 2). This figure follows the accuracy scores visualized in Figure 4.3.

In order to not reject the hypothesis that (H4) Cue and Target classes are separable from the Baseline class, the errors within Baseline-Cue and Baseline-Target need

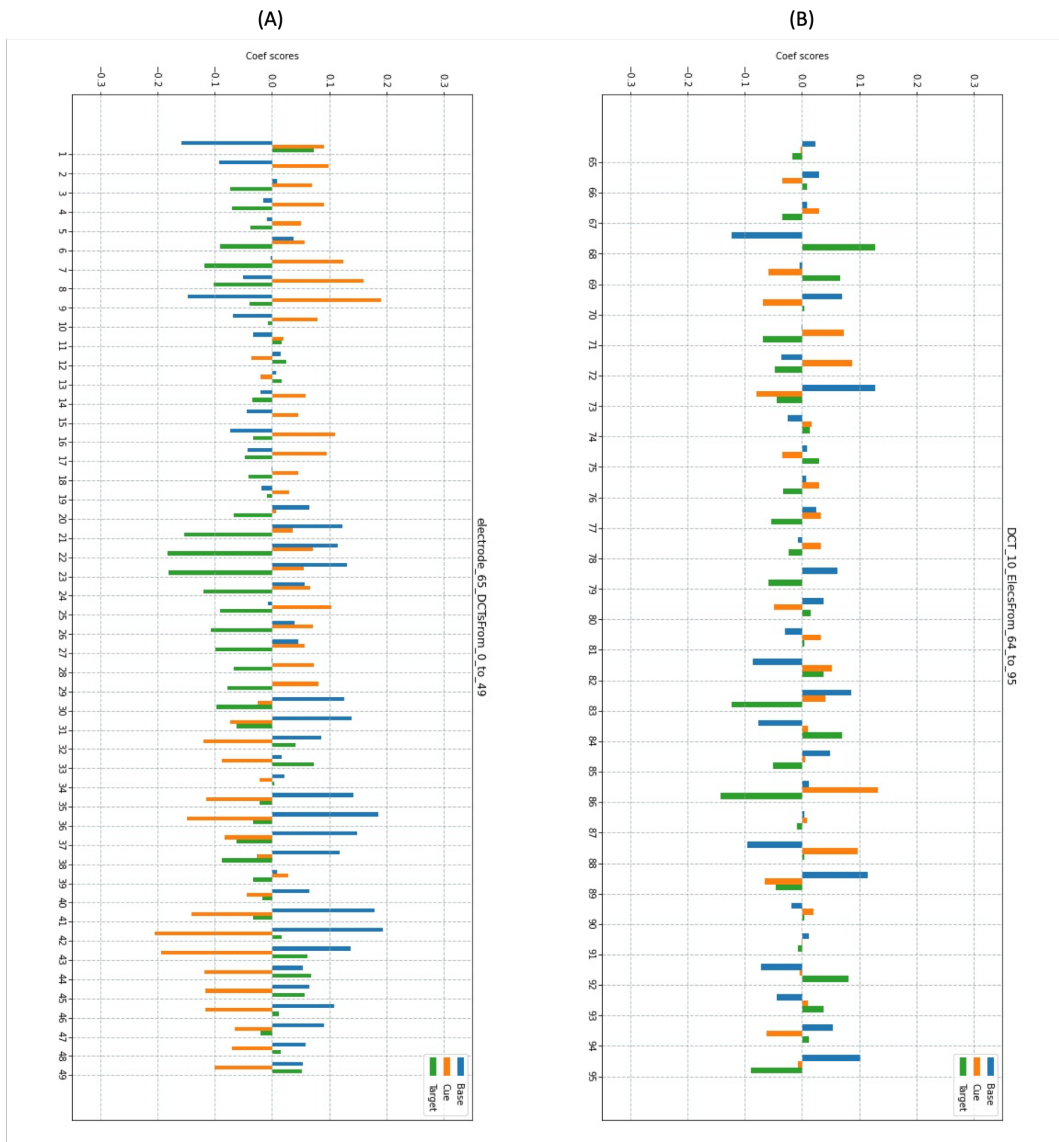


Figure 4.7: **Weight Coefficients of LR model:** Overview of trained LR model coefficient to look for patterns. Since there are 128×149 features, it is difficult to plot everything. Hence, we used two examples. Bar-plot (A) shows coefficients for DCT bin 10 for electrodes 64 to 95, and (B) shows coefficients for Electrode 65 for DCT 1 to 49.

to be smaller than the errors within Cue-Target. To do this, the confusion matrices are plotted. This is applied to both LR and SVM for top-performing DCT frequency ranges and N2PC regions.

R3.b: Analyse weight coefficients of learned models

The weight coefficients of each learned classifier (Baseline, Cue, Target) are plotted in order of DCT features and also in the order of electrodes. The purpose of this is

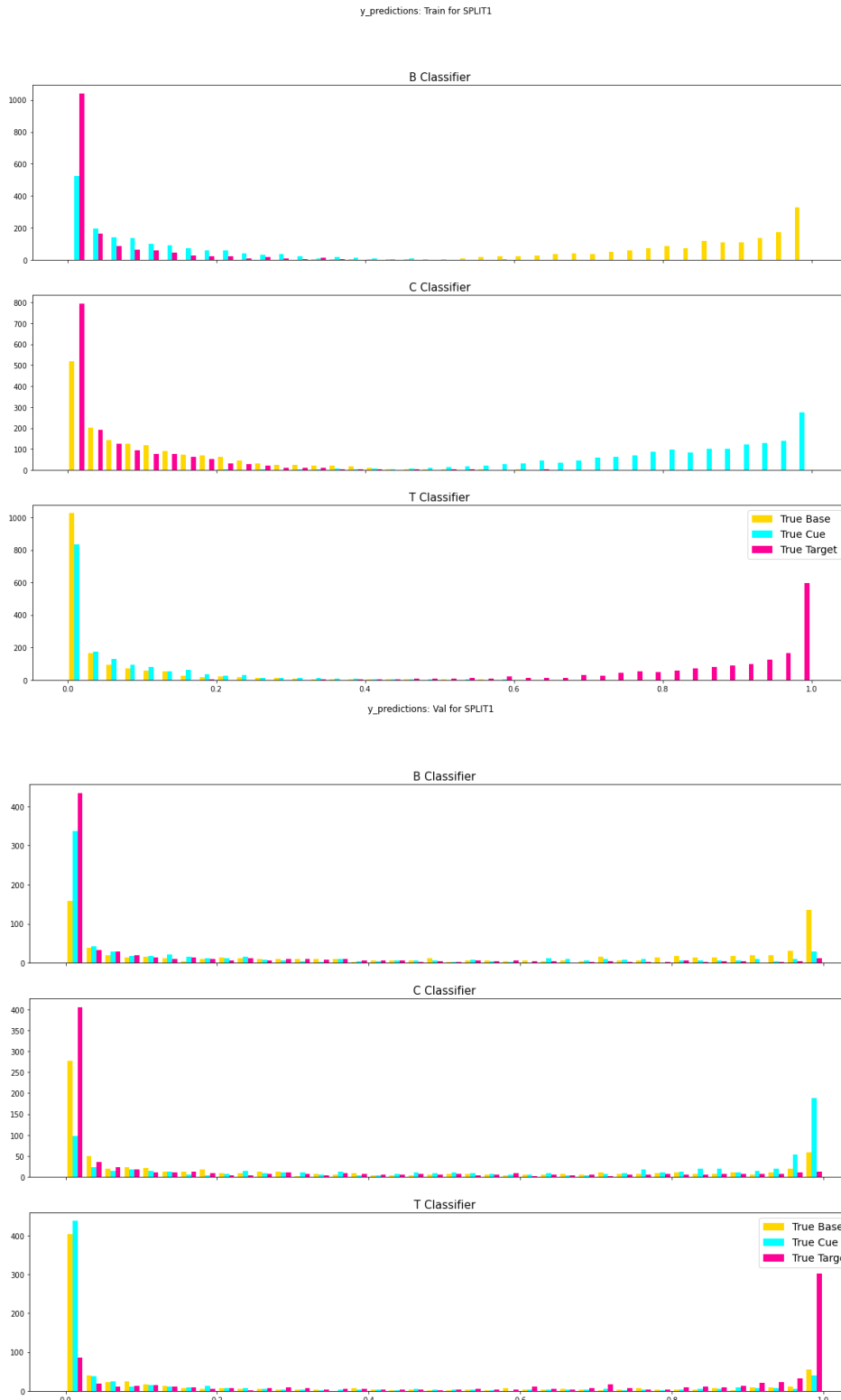


Figure 4.8: Classifier predictions for Baseline (Class 0), Cue (Class 1), and Target (Class 2). Top graph is training data, bottom graph is validation data.

to facilitate the view of patterns/analysis of the results. These results are shown in Figure. 4.7.

R3.c: Analyse prediction probability of learned classifiers

The prediction probabilities of the learned LR classifier were performed. The resulting classifier predictions are plotted in Figure 4.7, showing classifier prediction probabilities for Baseline (Class 0), Cue (Class 1), and Target (Class 2), for both the training set (top 3 subplots) and the validation set (bottom three subplots).

4.0.4 R4: Dimensionality Reduction to strengthen decisions to reject or not reject hypotheses

R4.a: LDA

The performance accuracy on the validation set for LR after applying LDA was 0.34. A random chance for a balanced dataset with three classes is 0.33. Results for LDA classification accuracy are shown in Figure 4.9. Training set performance is shown, as well.

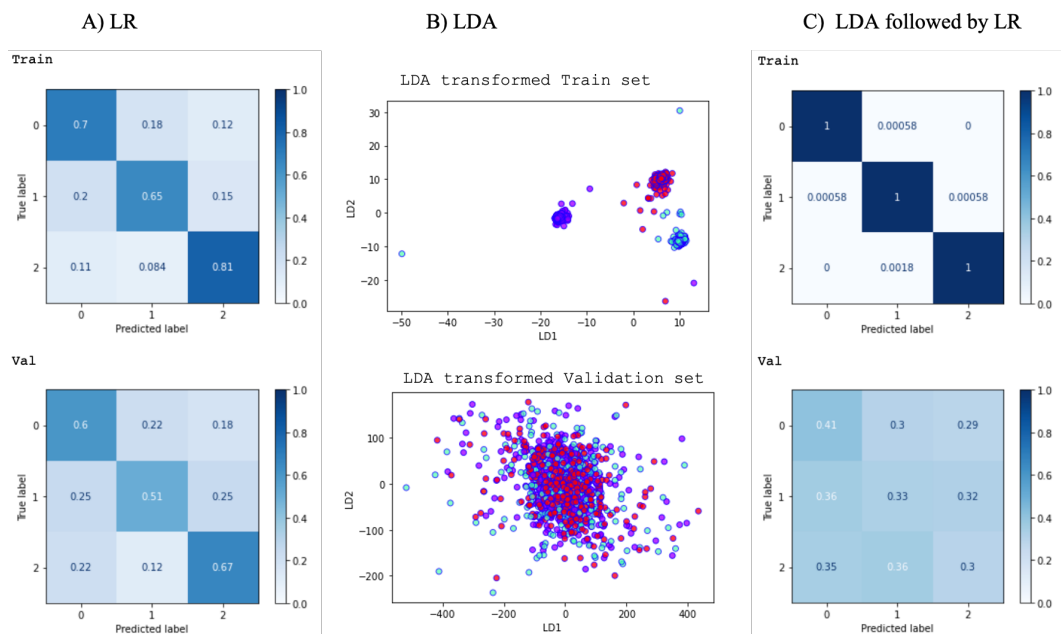
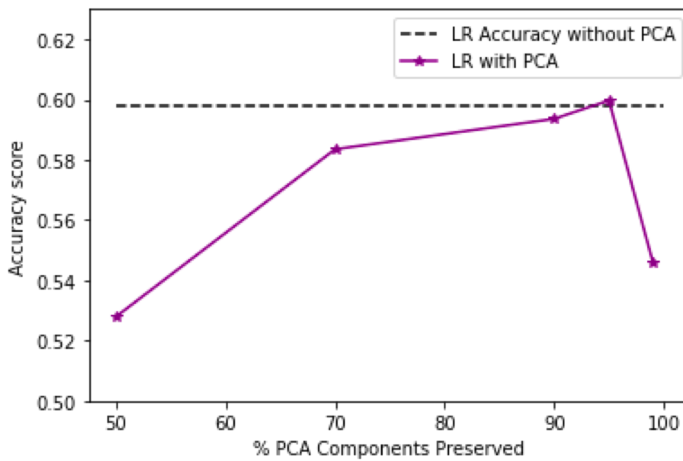


Figure 4.9: Figure showing LDA dimensionality reduction to training set (row 1) and validation set (row 2).

R4.b: PCA

PCA was applied to the dataset to decrease the dimensionality of the feature vector, in hopes that it will improve the accuracy score of the overall classification. For this, we varied the percent of PCA variances preserved and measures the accuracy score. PCA dimensionality reduction was applied to preserve 50, 70, 90, 95, and 98% of the variance. LR performance accuracy before and after PCA was reported. At 95% variances preserved, applying PCA transform before LR did improve the average accuracy by 0.001 (from 0.598 to 0.599). Figure 4.10 shows the accuracy scores over the percentage of the variances preserved.

(A) Loading Curve for Accuracy over % Components Preserved



(B) Confusion Matrices

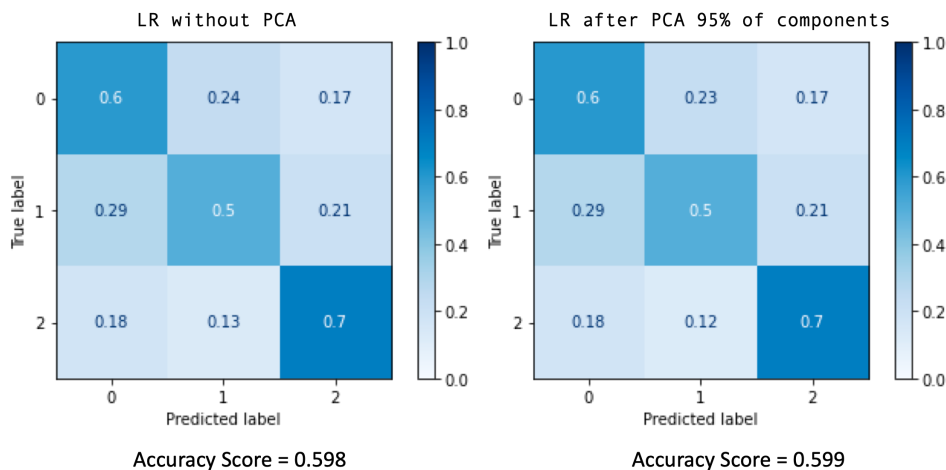


Figure 4.10: Figure showing PCA dimensionality reduction performance. (A) Accuracy scores on the validation set over various percentages of variances contained. (B) Confusion matrices for LR applied without (left) and with (right) PCA dimensionality reduction. Dotted black line is comparative LR performance accuracy.

Chapter 5

Discussions

This project aimed to understand if something as generic as paying attention to visual stimuli, whether intended or distractor objects, can be classified well using EEG neural data extracted DCT features. More clearly, the question was: is there a fast, objective method and distinguish types of attention? To accomplish this, ML techniques (Logistic Regression and Support Vector Classification) were applied to objectively determine the type of attention, without relying on subjective evaluation. To evaluate each experiment, model accuracy scores were used as a performance evaluation technique.

5.1 Hypotheses

To summarize the work-flow from the state of the art to the conclusion, a helpful illustration is shown in Figure 5.1, which highlights the working hypotheses. The four working hypotheses that have driven the work of this thesis are:

- H1: Selective attention is separable in the frequency domain.
- H2: N2PC regions hold most discriminative information.
- H3: Non-specific regions *do* hold discriminative information.
- H4: Baseline class (class 0) is separable from Distractor (class 1) and Intended (class 2) selective attention.

Section 5.2 discusses in detail the results obtained from the experiments and ties them back to the working hypotheses.

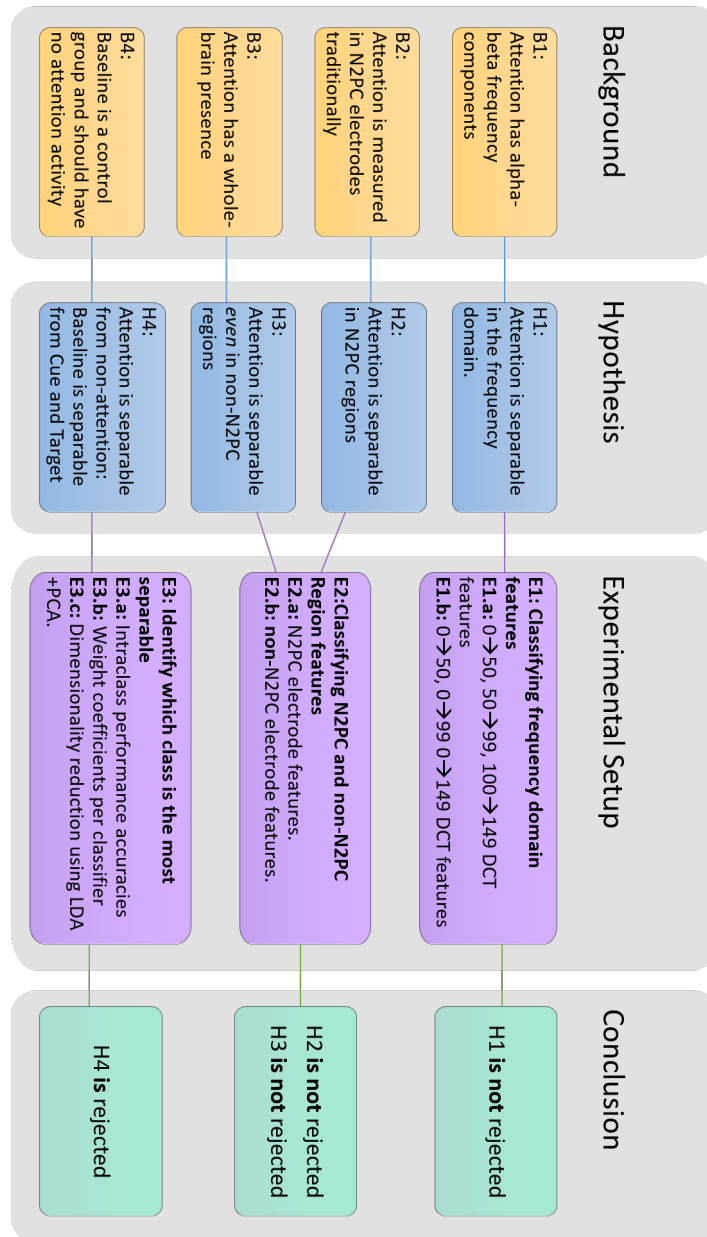


Figure 5.1: Figure illustrating the work-flow from background knowledge to rejecting or failing to reject the 4 hypotheses. The discussion of the experimental results which lead to the conclusions seen in this figure are explained in Section 5.2.

5.2 Discussion of Results

5.2.1 D1: Classifying frequency domain features

DCT 1:49 vs 59:99 and 100:149: The results from the experiments of the LR and SVM classifiers for DCT ranges of 1:49, 50:99, and 100:149 show that for ranges of 1 to 49 DCTs the performance accuracy is higher than for the other two ranges. As DCT 1:49 contained the selective attention relevant frequency oscillations, and

the features lead to a higher performance accuracy than the other feature ranges, the hypothesis that selective attention is separable in the frequency domain (H1) is not rejected.

DCT 1:49 vs 1:99 and 1:149: Additionally, the performance of the LR and SVM classifiers is lower for DCTs of 1 to 49 when compared to using 1 to 99 DCTs or 1 to 149 DCTs. This does not lead us to reject H1, as the selective attention frequency features are still contained in the three ranges for the second part of this experiment. H1 is not rejected.

5.2.2 D2: Classifying N2PC and non-N2PC Region features

N2PC: From the results of the N2PC feature classification experiments, N2PC region has the most discriminating information for classification. In addition to this, we were able to *contain* the 65 percent accuracy score even when only using 10.9 percent of the original number of electrodes by selecting electrodes associated with N2PC measures. This knowledge of selecting the correct features was following the N2PC state of the art [15, 18], which follows the electrodes indicated in Figure 3.5. Significantly decreasing the number of features while having little to no loss in accuracy scores is a significant result.

Non-N2PC: Although N2PC regions contain most information regarding the discriminability of types of attention, non-N2PC regions do indeed carry information relevant to discriminability for type attention. Given that change accuracy scores are 0.33 for the dataset, and accuracy of on average 0.4956 is 17 percent higher than chance, thus suggesting that discriminating information is indeed coded within non-N2PC electrodes and regions. Table 4.5 shows these values.

5.2.3 D3: Identify which class is the most separable

It was hypothesized that Baseline would separate better from Cue and Target, as the nature of the Baseline class does not contain selective attention data. By means of confusion matrices, analysis of the learned model, this hypothesis is tested.

Confusion matrices: Confusion matrices were calculated to portray the classification accuracy scored of each class in mean and standard deviation over a 10-fold cross-validation using GridSearchCV [8]. Since the errors within Baseline-Cue and Baseline-Target were larger than the errors within Cue-Target, H4 was rejected.

Weight Coefficients: Analysis on the weight coefficients of each learned classifier (Baseline, Cue, Target), either when plotted in order of DCT features and also in order of electrodes, lack a visible pattern. It is not possible to identify features

as consistently of high weight for a class, thus these features do not have high influence on the decision of the classifier. Since there is a lack of pattern in the weights, particularly between attention (Cue and Target) compared to non-attention (Baseline), H4 was rejected.

Prediction Probabilities: Errors in prediction probability of the true Baseline label should be lowest of the 3 labels in the Cue and Target classifiers, but the results show otherwise. Cue errors in prediction are much higher for Baseline than for Target. Since Cue or Target classifier predictions are higher at 1 for Baseline than for the other, H4 was rejected.

5.2.4 D4: Dimensionality Reduction to strengthen decisions to reject or not reject hypotheses

LDA: LDA did not perform well on the validation set. The resulting performance accuracy for LR post LDA transformation was significantly close to random change performance. This was expected, as the dataset had a very large dimension and a very small number of samples in comparison. LDA was able to find a direction that split the data best but resulted in over-fitting. In Figure 4.9, Training set performance is shown to highlight the likely over-fitting on the Train set.

PCA: PCA resulted in a good performance accuracy for LR post PCA transform using 90 % of variances. However, this could be a coincidence. Since the issue of high variance in the reported performance scores has been noticed, it would be necessary to apply PCA in a 10-fold cross validation.

5.3 Hypotheses rejected or not rejected

From the results of the experiments and the discussions above, the following conclusions have been reached:

- H1: Selective attention is separable in the frequency domain. **Not rejected**
- H2: N2PC regions hold most discriminative information. **Not rejected**
- H3: Non-specific regions *do* hold discriminative information. **Not rejected**
- H4: Baseline class (class 0) is separable from Distractor (class 1) and Intended (class 2) selective attention. **Rejected**

5.3.1 Discussions Summary

Although employing DCT as a feature extraction procedure is an ideal candidate for extracting frequency components from signals, the frequencies components held within DCT bins were not reflective of the desired frequency information. This is likely due to the DCT bins not holding small enough frequency increments for the alpha and beta oscillations.

However, DCT for feature extraction did extract relevant selective attention information, particularly from the ranges that were expected. Using all of the DCT frequency features resulted in the best accuracy score of 0.65. As the resulting performance accuracy of 0.65 was as high as other reported results[17, 46]. Thus, this makes making the resulting performance accuracy comparable with other selective attention results (see Table 5.1).

Classification				
Group	Classes	Feature	Accuracy Score	Topic
Fanda et al (us)	3	DCT	0.65	Attention
Wen et al [46]	2,3	MEG Amplitude	0.74, 0.65-0.67	Attention
Fahrenfort et al [17]	2	EEG Amplitude	0.65	Attention

Table 5.1: Table of Classification Accuracy score summaries, between other selective attention studies, as well as other BCI and Epilepsy classification studies.

From Figure 4.5 and Table 4.1, the results suggest that classifying selective attention with only 14 N2PC electrodes and all DCTs at best performance is only, on average, 0.02 weaker in accuracy scores than with all 128 electrodes. The figure suggests that the best GridSearchCV value should be taken with a grain of salt, as it does not show the variability in the accuracy score, which is important when variance is large in the reported 10-fold cross-validation accuracy scores.

Additionally, indeed, selective attention is a whole brain process. This was suggested by the analysis of non-N2PC region classification accuracy scores. Although the accuracy scores of non-N2PC region electrodes were, on average, 0.10 less than the accuracy scores of N2PC regions, the accuracy scores were higher than 0.33, indicating that there is discriminative information about classifying attention to distractors or intended objects even in non-N2PC regions.

Comparing Experiment Results

As mentioned above, the best accuracy score reported was 0.65 when all features were used, with both LR and SVM. To compare each of the experiments, Table 5.2

is created. In addition to average performance and max performance, the table shows a ranking of the performances first by max performance, then by average performance. From this, the second-best performance accuracy comes from the use of N2PC features followed by DCT 1:49 as third-best performance accuracy.

Experiment Classification			
Features	Average Performance	Max Performance	ranking
All features	0.5992 SVM	0.65 SVM/LR	1
1.a DCT 1:49	0.5190 SVM	0.60 SVM	3
2.a N2PC	0.5850 LR	0.65 SVM	2
2.b Non-N2PC	0.4865 SVM	0.53 SVM	4
4.b PCA (*0.95)	0.5990 LR	N/A	N/A

Table 5.2: Table of Experimental results of classification performance accuracy across the experimental setups. For PCA, (*0.95) indicates 0.95 of the variance contained.

5.3.2 Limitations:

Although the performance accuracies are comparable to classification performances of other selective attention tasks, there are still limitations to consider. This includes, but is not limited to, features, data scarcity, population sampling, and experiment limitations. This subsection will explain in more detail each limitation.

Features:

This thesis was limited to only using DCT features, and would have benefited from comparing performances of the algorithms by using features such as raw EEG, smoothed EEG amplitude and other statistical values of the EEG signal, and other frequency features (non-DCT). Additionally, the use of additional data collection methods can likely improve the performance, although EEG is a state-of-the-art device for traditional selective attention analysis.

Data scarcity:

An important finding in this thesis was the high variance in performance accuracy from the 10-fold cross-validation. To recall, each different split of participants lead to roughly 10 percent variance in performance accuracy. To decrease this variance in performance, the algorithm should be trained in datasets that are a more complete representation of the population. This way, the algorithm can perform with more consistent accuracy and less variance in performance accuracy.

Experiment limitations:

The data used for the classification of selective attention comes from a very specific but honed paradigm that evokes selective attention in participants. Within this paradigm, there are 2 additional conditions that also use audio stimulation and two other conditions. To increase the generalizability of the current solution on classifying responses, it would be beneficial to incorporate other stimuli. In neuroscience terms, the analysis could benefit from the classification of brain responses to target-matching (TCCV) vs non-target matching (NCCV or TCCAV) distractors.

Population sampling:

For the purpose of the study, the population sampling was opportunistic, across university students, graduate students, and young professionals within Switzerland. Although this is a common method for data collection across neuroscience studies, it is nonetheless a limitation.

5.4 Conclusion

People's ability to behave effectively in everyday situations is critically dependent on "selective attention", which is the ability to promote the processing of objects that match our current behavioural goals and suppress those objects that do not match those goals. The aim of this project was to classify these two task-oriented processes.

Aims

The results showed the classification accuracy for classifying selective attention with only 14 N2PC electrodes is only, on average, 0.02 weaker in accuracy scores than with all 128 electrodes. This is a minimal loss in performance in comparison to only using 10 percent of the original electrodes.

Additionally, the results showed that, indeed, selective attention is a spatially spread process. This was suggested by the analysis on non-N2PC region classification accuracy scores. Although the accuracy scores of non-N2PC region electrodes were on average of about 0.10 less than the accuracy scores of N2PC regions, the accuracy scores were higher than 0.33, indicating that there is discriminative information about classifying attention to distractors or intended objects even in non-N2PC regions.

Improvements

The last decades have provided important advances in terms of brain and cognitive mechanisms orchestrating selective attention as well as their role in enhancing perception and supporting the learning of new information. Additionally, the last decades have shown a lot of important advances in ML applications. It would be beneficial to further integrate the two fields, filling the gaps of reviews, algorithm performance tests, etc. on attention data.

Although DCT feature extraction performed reasonably, the feature extraction method could still be improved. Employing another frequencies feature extraction method could possibly split the alpha and beta oscillations better, thus creating bins with higher sensitivity to the alpha and beta frequencies, could lead to better performance.

Moreover, using automatic feature selection techniques would be very beneficial for biological data, in particular for signals of complex nature, such as attention, as they are "Unseen" mechanisms and can benefit from unsupervised exploration. For this reason as well it would be particularly useful to model and understand cognition processes through means of AI application on selective attention data.

Exit thoughts

The aim of this project was to understand if paying attention to visual stimuli, whether intended or distracted, can be classified well. For the purpose of the aims, the results suggest that attention to intended objects and distractor objects can be classified, although not with high confidence.

Although a performance accuracy of 0.59 on average and 0.65 at best is not a very good accuracy score for a model performance, is it better than chance (0.33 for a balanced class problem). It is possible that, with improvements in preprocessing, other feature extraction methods, and more experiments, this performance could increase.

N2PC is valuable, as involuntary vs. voluntary attention informs us about the distractors' ability to diverge attentional control. Understanding the bio-markers of voluntary and involuntary attention, and distinguishing each other, could possibly help understand earlier on flags for attentional dynamics.

Bibliography

- [1] Fiorenzo Artoni, Arnaud Delorme, and Scott Makeig. “Applying dimension reduction to EEG data by Principal Component Analysis reduces the quality of its subsequent Independent Component decomposition”. In: *NeuroImage* 175 (2018), pp. 176–187.
- [2] Sylvain Baillet, Karl Friston, and Robert Oostenveld. *Academic software applications for electromagnetic brain mapping using MEG and EEG*. 2011.
- [3] Md Khayrul Bashar et al. “Epileptic seizure classification from intracranial EEG signals: A comparative study EEG-based seizure classification”. In: *2016 IEEE EMBS Conference on Biomedical Engineering and Sciences (IECBES)*. IEEE. 2016, pp. 96–101.
- [4] Marisa Carrasco. “Visual attention: The past 25 years”. In: *Vision research* 51.13 (2011), pp. 1484–1525.
- [5] Vincent P Clark, Silu Fan, and Steven A Hillyard. “Identification of early visual evoked potential generators by retinotopic and topographic analyses”. In: *Human brain mapping* 2.3 (1994), pp. 170–187.
- [6] Maurizio Corbetta and Gordon L Shulman. “Control of goal-directed and stimulus-driven attention in the brain”. In: *Nature reviews neuroscience* 3.3 (2002), pp. 201–215.
- [7] Jennifer T Coull and Anna C Nobre. “Where and when to pay attention: the neural systems for directing attention to spatial locations and to time intervals as revealed by both PET and fMRI”. In: *Journal of Neuroscience* 18.18 (1998), pp. 7426–7435.
- [8] *Cross-Validation Grid Search: sklearn*. https://scikit-learn.org/stable/modules/generated/sklearn.model_selection.GridSearchCV.html?highlight=gridsearchcv#sklearn.model_selection.GridSearchCV. Accessed: 2020-06-30.
- [9] John P Cunningham and M Yu Byron. “Dimensionality reduction for large-scale neural recordings”. In: *Nature neuroscience* 17.11 (2014), pp. 1500–1509.
- [10] Cathy N Davidson. *Now you see it: How the brain science of attention will transform the way we live, work, and learn*. Viking New York, NY, 2011.

- [11] *Definition of Attentional Blindness by the American Psychology Association*. <https://dictionary.apa.org/attentional-blindness>. Accessed: 2020-10-30.
- [12] Robert Desimone and John Duncan. "Neural mechanisms of selective visual attention". In: *Annual review of neuroscience* 18.1 (1995), pp. 193–222.
- [13] Francesco Di Russo et al. "Cortical sources of the early components of the visual evoked potential". In: *Human brain mapping* 15.2 (2002), pp. 95–111.
- [14] *Discrete Cosine Transform*. <https://docs.scipy.org/doc/scipy/reference/generated/scipy.fftpack.dct.html>. Accessed: 2020-06-30.
- [15] Martin Eimer. "The N2pc component as an indicator of attentional selectivity". In: *Electroencephalography and clinical neurophysiology* 99.3 (1996), pp. 225–234.
- [16] *ERP markers of target selection discriminate children with high vs. low working memory capacity*. <https://www.ncbi.nlm.nih.gov/pmc/articles/PMC4633470/>. Accessed: 2020-12-16.
- [17] Johannes Jacobus Fahrenfort et al. "Multivariate EEG analyses support high-resolution tracking of feature-based attentional selection". In: *Scientific reports* 7.1 (2017), pp. 1–15.
- [18] Charles L Folk, Roger W Remington, and James C Johnston. "Involuntary covert orienting is contingent on attentional control settings." In: *Journal of Experimental Psychology: Human perception and performance* 18.4 (1992), p. 1030.
- [19] Deon Garrett et al. "Comparison of linear, nonlinear, and feature selection methods for EEG signal classification". In: *IEEE Transactions on neural systems and rehabilitation engineering* 11.2 (2003), pp. 141–144.
- [20] DA Jeffreys and JG Axford. "Source locations of pattern-specific components of human visual evoked potentials. I. Component of striate cortical origin". In: *Experimental brain research* 16.1 (1972), pp. 1–21.
- [21] Matthias Kaper et al. "BCI competition 2003-data set IIb: support vector machines for the P300 speller paradigm". In: *IEEE Transactions on biomedical Engineering* 51.6 (2004), pp. 1073–1076.
- [22] Seyed Mostafa Kia, Emanuele Olivetti, and Paolo Avesani. "Discrete cosine transform for MEG signal decoding". In: *2013 International Workshop on Pattern Recognition in Neuroimaging*. IEEE. 2013, pp. 132–135.
- [23] Monika Kiss, José Van Velzen, and Martin Eimer. "The N2pc component and its links to attention shifts and spatially selective visual processing". In: *Psychophysiology* 45.2 (2008), pp. 240–249.
- [24] Monika Kiss et al. "Attentional capture by salient distractors during visual search is determined by temporal task demands". In: *Journal of cognitive neuroscience* 24.3 (2012), pp. 749–759.

- [25] Wolfgang Klimesch. "Alpha-band oscillations, attention, and controlled access to stored information". In: *Trends in cognitive sciences* 16.12 (2012), pp. 606–617.
- [26] *Linear Discriminate Analysis: sklearn*. https://scikit-learn.org/stable/modules/lda_qda.html#dimensionality-reduction-using-linear-discriminant-analysis. Accessed: 2020-06-30.
- [27] *Logistic Regression: sklearn*. https://scikit-learn.org/stable/modules/generated/sklearn.linear_model.LogisticRegression.html#sklearn.linear_model.LogisticRegression. Accessed: 2020-06-30.
- [28] Fabien Lotte et al. "A review of classification algorithms for EEG-based brain-computer interfaces". In: *Journal of neural engineering* 4.2 (2007), R1.
- [29] Fabien Lotte et al. "A review of classification algorithms for EEG-based brain-computer interfaces: a 10 year update". In: *Journal of neural engineering* 15.3 (2018), p. 031005.
- [30] Pawel J Matusz et al. *Are we ready for real-world neuroscience?* 2019.
- [31] *MNE Tools*. <https://mne.tools/stable/index.html>. Accessed: 2020-06-30.
- [32] Dirk van Moorselaar and Heleen A Slagter. "Learning what is irrelevant or relevant: Expectations facilitate distractor inhibition and target facilitation through distinct neural mechanisms". In: *Journal of Neuroscience* 39.35 (2019), pp. 6953–6967.
- [33] Micah M Murray et al. "The multisensory function of the human primary visual cortex". In: *Neuropsychologia* 83 (2016), pp. 161–169.
- [34] Micah M Murray et al. "Visuo-spatial neural response interactions in early cortical processing during a simple reaction time task: a high-density electrical mapping study". In: *Neuropsychologia* 39.8 (2001), pp. 828–844.
- [35] *Niedermeyer's Electroencephalography: Basic Principles, Clinical Applications, and Related Fields (7 ed.)* <https://oxfordmedicine.com/view/10.1093/med/9780190228484.001.0001/med-9780190228484>. Accessed: 2020-12-16.
- [36] Mohammad Zavid Parvez and Manoranjan Paul. "Features extraction and classification for Ictal and Interictal EEG signals using EMD and DCT". In: *2012 15th International Conference on Computer and Information Technology (ICCIT)*. IEEE. 2012, pp. 132–137.
- [37] Fabian Pedregosa-Izquierdo. "Feature extraction and supervised learning on fMRI : from practice to theory". Theses. Université Pierre et Marie Curie - Paris VI, Feb. 2015. URL: <https://tel.archives-ouvertes.fr/tel-01100921>.

- [38] Gert Pfurtscheller et al. "EEG-based discrimination between imagination of right and left hand movement". In: *Electroencephalography and clinical Neurophysiology* 103.6 (1997), pp. 642–651.
- [39] Alois Schlögl et al. "Characterization of four-class motor imagery EEG data for the BCI-competition 2005". In: *Journal of neural engineering* 2.4 (2005), p. L14.
- [40] *Scikit Learn*. <https://scikit-learn.org/stable/>. Accessed: 2020-12-16.
- [41] *Scikit Learn PCA Decomposition*. <https://scikit-learn.org/stable/modules/generated/sklearn.decomposition.PCA.html>. Accessed: 2020-12-16.
- [42] Paul Scotti et al. "EduCortex: browser-based 3D brain visualization of fMRI meta-analysis maps". In: *Journal of Open Source Education* 3.26 (2020), p. 75.
- [43] *Support Vector Classification: sklearn*. <https://scikit-learn.org/stable/modules/generated/sklearn.svm.SVC.html#sklearn.svm.SVC>. Accessed: 2020-06-30.
- [44] Nora Turoman. "Early multisensory attention as a foundation for learning in multicultural Switzerland". PhD thesis. 2020. URL: https://serval.unil.ch/en/notice/serval:BIB_324C94948ED2.
- [45] Nora Turoman et al. "The development of attentional control mechanisms in multisensory environments". In: *bioRxiv* (2020).
- [46] Tanya Wen, John Duncan, and Daniel J Mitchell. "The time-course of component processes of selective attention". In: *NeuroImage* 199 (2019), pp. 396–407.
- [47] Yingjie Zhang et al. "The Research of the Feature Extraction and Classification Algorithm Based on EEG Signal of Motor Imagery". In: *2019 International Conference on Virtual Reality and Intelligent Systems (ICVRIS)*. IEEE. 2019, pp. 187–190.

Lora Fanda, M.Sc.

Curriculum Vitae, Aug 2020

Sierre
Switzerland
☎ +41 76 566 47 55
✉ lorafanda@gmail.com
🌐 www.lorafanda.com

Work

- Since Aug'20 **Research Assistant**, *University of Applied Science Western Switzerland (HES-SO)*, Sierre, CH
Research Areas: Selective Attention, EEG Data Analysis, Cognitive Neuroscience, Clinical Research
Supervisor: Dr. Pawel Matusz.
- Aug'19–Jul'20 **Research Assistant**, *Fondation Asile des Aveugles (FAA); (HES-SO)*, Lausanne, CH
Research Areas: Amblyopia, EEG Data Analysis, Cognitive Neuroscience, Clinical Research
Supervisor: Dr. Micah Murray.
- Sep'17–Mar'19 **Research Data Associate**, *FlinkerLab*, NYU Langone Medical Center, NYC, New York, USA
Research Areas: Google Project, Princeton Project, ECoG Data Analysis, Epilepsy, Clinical Research
Supervisor: Dr. Adeen Flinker.
- Jul'17–Aug'17 **Undergraduate Research Assistant**, *CWRU Department of Biomedical Engineering*, Cleveland, Ohio, USA
Research Areas: Deep-learning classification, Lung cancer, digitized stained tissue slides.
Supervisor: Dr. Anant Madabhushi.
- Jan'13–Jun'17 **Tutor**, *Passaic County Community College (PCCC)*, Paterson, New Jersey, USA – (*part-time*)
Topics: Calculus, Physics, Biology, Chemistry.
- Jun'16–Dec'16 **System Verification Engineer**, *Philips Healthcare Systems - North America*, Cleveland, Ohio, USA
Work Area: CT Scan Tests, FDA Procedure, Verification Engineering.
- Dec'15–Aug'16 **Undergraduate Research Assistant**, *CWRU Department of Biomedical Engineering*, Cleveland, Ohio, USA
Research Areas: Device Design, sEMG Data Analysis, Grant Writing, Prototyping.
Supervisor: Dr. Abidemi Ajiboye.

Education

- Jan'19–Sep'20 **M.Sc. in Artificial Intelligence (AI)**,
IDIAP, Research Institute / Swiss Distance Learning University, Martigny, Switzerland,
Topics: Neural Signal Classification, Selective Attention, Cognitive Neuroscience.
Thesis: Thesis: Classifying Attentional Dynamics in Adults from Electroencephalography (EEG) signals.
Supervisors: Dr. André Anjos; Dr. Pawel Matusz.
- Sep'13–Aug'17 **B.Sc. in Biomedical Engineering**, *minor: Electrical Engineering*,
Case Western Reserve University, Cleveland, Ohio, U.S.,
Topics: Biomedical Devices and Instrumentation, Biomedical Analysis.
Thesis: Surface Electromyographic (sEMG) control of a smartphone.
Supervisor: Prof. Andrew Rollins.

Awards - Grants

- Awards: **Leadership**, "Student Leadership Award for Group Community Service". *MIND Group*, Vice-President, Dec 2015.
Academic Award, *Phi Theta Kappa (PTK) Honors Society*, at PCCC, May 2012.
- Grants: **Case Western Reserve University**, "Student Project Fund Recipient", Think[box] Foundation, Sep 2017.

Internships & Additional Training

- Jun'16–Dec'16 **System Verification Engineer Internship**, *Philips Healthcare Systems*, Cleveland, Ohio, U.S.
Aug'16 **Medical Imaging Summer School**, *University of Catania*, Favignana, Italy.

Research Projects

- 2019 **AMBER**, ([link](#)), Data Analyst, HES-SO, Switzerland.
- 2017 **24/7 Project**, *Data Acquisition and Analyst, Neural Analysis for Predicting Cognition*, Google, New York City, U.S.; Princeton University (Hasson Lab), Princeton, U.S.
- 2015 **Music in Motion**, ([link](#)) *Designer and Developer*, Case Western Reserve University, Cleveland, Ohio, U.S.

Workshops [W] and Seminars [S]

- Jul 2019 **[S]: The Importance of Curiosity and Education**, *STEM Summer Scholars Academy, PCCC, Paterson, U.S.*
- Jul 2018 **[S]: The Importance of Curiosity and Education**, *STEM Summer Scholars Academy, PCCC, Paterson, U.S.*
- Jul 2018 **[W]: Signal Processing Workshop for Bioelectric Signals**, *Princeton University, Princeton, U.S.*

Languages

English, Albanian, Turkish, Macedonian: - Native, **French**: - B2.

Social Engagements [SE] and Hobbies [H]

[SE]: • Medical Instruments for Nations under Development, (2014 – 2017); • Volleyball Trainer/Coach

[H]: • Volleyball • Skiing • Painting • Biking • Traveling

References

Person	Role	Institute	contact
○ Dr. Adeen Flinker	Head of Flinker Lab	NYU Langone Medical Center	adeen.flinker@nyulangone.org
○ Dr. Pawel Matusz	MSc Supervisor	HES-SO, Valais/Wallis	pawel.matusz@hevs.ch
○ Prof. Uri Hasson	Head of Hasson Lab	Princeton University	hasson@princeton.edu

Publications

Journal Papers

Shum J, [Fanda L](#), Dugan P, Doyle W, Devinsky O, Flinker A. *Neural correlates of sign language production revealed by electrocorticography*. Neurology Aug 2020. DOI: 10.1212/WNL.0000000000010639

Conference Papers

Simon-Martinez C, Turoman N, [Fanda L](#), Matusz P. *Can children improve their attention skills in multisensory environments during a single session?* Swiss Society for Early Childhood Research. Nov 2020.

Goldstein A, Jansen A, Slaney M, Price A, Zada Z, Choe G, Aubrey B, Rao A, [Fanda L](#), Norman K, Flinker A, Devinsky O, Brenner M, Hasson U. *Temporal Dynamics of Meaning*. Cognitive Computational Neuroscience, Jan 2019.

Undergraduate Abstracts

[Fanda L](#), Nieto S, Patel J, Spessert E. *Surface Electromyographic (sEMG) control of a smartphone*. Case Western Reserve University, Undergraduate Research Conference. May, 2017.

Conference Abstracts

Shum J, Mahmood B, [Fanda L](#), Dugan P, Friedman D, Doyle W, Devinsky O, Flinker A. *Functional Mapping of Language with High Gamma Electrocorticography*. Society for Neuroscience, Chicago, October 2019.

Shum J, [Fanda L](#), Mahmood B, Friedman D, Dugan P, Doyle W, Devinsky O, Flinker A. *Neural correlates of American Sign Language production revealed by electrocorticography*. Society for the Neurobiology of Language. Helsinki, Finland, August 2019.

Shum J, Mahmood B, [Fanda L](#), Friedman D, Dugan P, Doyle W, Devinsky O, Flinker A. *Functional mapping of language with high gamma electrocorticography using a battery of five language tasks*. NYU Neurology Research Symposium. May 15 2019.

Shum J, Mahmood B, [Fanda L](#), Dugan P, Friedman D, Doyle W, Devinsky O, Flinker A. *Functional mapping of language with high gamma electrocorticography using a battery of five language tasks*. NYU Neuroscience Retreat, April 5 2019.

Shum J, Mahmood B, [Fanda L](#), Friedman D, Dugan P, Doyle W, Devinsky O, Flinker A. *Functional mapping of language with high gamma electrocorticography compared with electrical brain stimulation*. American Epilepsy Society. AES 2018 Conference New Orleans, December 2018

Shum J, [Fanda L](#), Mahmood B, Friedman D, Dugan P, Doyle W, Devinsky O, Flinker A. *Neural correlates of sign language and spoken language revealed by electrocorticography*. Society for Neuroscience, San Diego, November 2018.

Ozker M, McAlister M, [Fanda L](#), Mahmood B, Dugan P, Friedman D, Doyle W, Devinsky O, Flinker A. *Intracranial neurophysiology of auditory feedback control during speech production*. Society for Neuroscience, San Diego, November 2018.

Ozker M, McAlister M, [Fanda L](#), Shum J, Dugan P, Friedman D, Doyle W, Devinsky O, Flinker A. *Neural correlates of delayed auditory feedback during speech production investigated by electrocorticography*. Society for Neuroscience, San Diego, November 2018.

Shum J, [Fanda L](#), Mahmood B, Friedman D, Dugan P, Doyle W, Devinsky O, Flinker A. *Neural correlates of sign language and spoken language revealed by electrocorticography*. Society for Neuroscience, San Diego, November 2018.

Shum J, [Fanda L](#), Friedman D, Dugan P, Devinsky O, Flinker A. *Neural correlates of sign language and spoken language revealed by electrocorticography*. NYU Neurology Research Symposium. May 16 2018.